DEVELOPMENT OF MULTI-YEAR LAND COVER DATA TO ASSESS WILDFIRE IMPACTS TO COASTAL WATERSHEDS AND THE NEARSHORE ENVIRONMENT

A Thesis

Presented in Partial Fulfillment of the Requirement for the

Degree of Master of Science

with a

Major in Geography

in the

College of Graduate Studies

University of Idaho

by

Katherine D. Morrison

May 2014

Major Professor: Crystal A. Kolden, Ph.D.

Authorization to Submit Thesis

This thesis of Katherine D. Morrison, submitted for the degree of Master of Science with a Major in Geography and titled "Development of multi-year land cover data to assess wildfire impacts to coastal watersheds and the nearshore environment" has been reviewed in final form. Permission, as indicated by the signatures and dates below, is now granted to submit final copies to the College of Graduate Studies for approval.

Major Professor:	_____	Date:	_____
	Crystal A. Kolden, Ph.D.		
Committee Members:	_____	Date:	_____
	Jeffrey Hicke, Ph.D.		
	_____	Date:	_____
	Philip Higuera, Ph.D.		
Department Administrator:	_____	Date:	_____
	Karen Humes, Ph.D.		
Discipline's College Dean:	_____	Date:	_____
	Paul Joyce, Ph.D.		

Final Approval and Acceptance

Dean of the College of Graduate Studies:	_____	Date:	_____
	Jie Chen, Ph.D.		

Abstract

In the Mediterranean ecosystems of coastal California, wildfire is a common disturbance that can significantly alter vegetation in watersheds that transport sediment and nutrients to the adjacent nearshore oceanic environment. We assess the impact of two wildfires that burned in 2008 on land cover and to the nearshore environment along the Big Sur coast in central California. We created a multi-year land cover dataset to assess changes to coastal watersheds as a result of fire. This land cover dataset was then used to model changes in nonpoint source pollutants transported to the nearshore environment. Results indicate post-fire increases in percent export compared to pre-fire years, and also link wildfire severity to specific land cover changes that subsequently increase exports of pollutants and sediment to the nearshore environment. This approach is replicable across watersheds and also provides a framework for including the nearshore environment as resource worth protecting for terrestrial land management involving wildfire, including suppression, thinning, and other activities that alter land cover at a landscape scale.

Acknowledgements

I would first like to acknowledge my advisor, Dr. Crystal A. Kolden, for her considerable time and effort put forth to improve the quality and content of this thesis. I also owe a debt of gratitude to Dr. Kolden for her willingness to support my research during my time spent at the University of Idaho. Thank you also to my committee members Dr. Jeffrey Hicke and Dr. Philip Higuera for their time and feedback. In addition, I would especially like to thank Vincent Jansen for his help with field work and for being a continual sounding board, and many other colleagues who provided feedback and guidance, including: Collette Gantenbein, Brandon Moore, and Arjan Meddens. I would also like to thank my wonderful family and friends for their enduring support and comic relief over the last few years. Finally, this research was made possible through grants funded through Idaho EPSCoR and the Department of Geography.

Dedication

For my Dad, my first and greatest teacher

Table of Contents

Authorization to Submit Thesis ii
Abstract iii
Acknowledgements iv
Dedication v
List of Figures viii
List of Tables ix
Chapter 1: Using a decision tree to create a historical multi-year land cover classification 1
Abstract 1
1. Introduction 1
2. Methods 5
2.1. Study Area 5
2.2. Satellite and Ancillary Data 6
2.3. Classification Scheme & Reference Data 7
2.4. Classification Tree 9
2.5. Accuracy Assessment 9
3. Results 10
3.1. Classification Tree 10
3.2. Classification Accuracy 10
4. Discussion 11
5. Conclusion 14
Figures and Tables 15
References 24
Chapter 2: Impacts of wildfire on coastal watersheds and the nearshore environment in Big Sur, California 29
Abstract 29
1. Introduction 29
2. Methods 34
2.1. Study Area 34
2.2. Fire Effects 35

2.4. Hydrologic Effects 38
2.5. Analysis 40
3. Results 41
3.1. Land cover 41
3.2. Watershed Outputs 42
3.3 Burn severity and watershed export 42
4. Discussion 43
5. Management Implications 48
6. Conclusion 49

List of Figures

Figure 1.1. Big Sur region of the central California coast, and the 2008 Basin Complex and Chalk fires 15

Figure 1.2. Classification tree for base year 2012 which was applied to all years 16

Figure 1.3. Maps of spatial distribution of accuracy for 2012 shrub cover. Values represent the probability of the presence of the correct class. Maps of agreement between reference data and classified map for 2012. Solid circles represent agreement in both data sets, unfilled circles represent shrub points incorrectly classified as forest or grass (omission error), and the crosses represent forest or shrub points incorrectly classified as shrub (commission error)..... 17

Figure 2.1. Basins and sample points in the Big Sur region of coastal central California. Burned basins are in bold..... 50

Figure 2.2. Burned and unburned land cover transitions in (a.) forest, (b.) shrub, and (c.) grass cover over the study period (2005 – 2012). Envelopes represent the average error of commission as a percent for each class 51

Figure 2.3. Percent change in nonpoint source pollutants based on pre-fire average (2005 – 2007) for both burned and unburned basins. Within burned areas, 2008 includes only the burned basins and pre-fire baselines affected by the Basin Complex fire 52

Figure 2.4. OpenNSPECT pollutant concentration estimation process (NOAA 2012). Shading represents output dataset 53

Figure 2.5. Distributions of dNBR per land cover transition. FG = forest to grass, FS = forest to shrub, and SG = shrub to grass 55

List of Tables

Table 1.1. Sensor name and date of acquisition for remotely sensed 18

Table 1.2. Spectral and ancillary input variables 19

Table 1.3. Land cover classes based on the descriptions used for the National Land cover Dataset (NLCD) 20

Table 1.4 Reference data obtained for classification. NAIP sources were photointerpreted from a point grid over the study area. Persistent sites consist of photointerpreted sites that remained constant from 2005 through 2009 and 2012. 2012 sites were divided into training (75 percent) and validation (25 percent), for all other years, sites were used for validation 21

Table 1.5. Classification error matrices for each year 22

Table 1.6. Quartiles for geographically weighted logistic regression representing probability of the classification correctly predicting the 2012 reference data. Interquartile range (IQR) represents the variability in probability 23

Table 2.1. Basins within the study area from north to south and fire impacts including fire name, percent area burned, percent high severity (calculated as percent high severity of percent area burned), and Severity Metric (SM). Basins in bold are considered to be the burned basins for analysis and were > 75 % burned 56

Table 2.2 Spearman Rank correlations (r) between fire metrics and percent changes in modeled annual concentrations of nonpoint source pollutants for the two periods of post-fire year 0 (2006 – 2008) and post-fire year 1 (2006 – 2009). Values in bold are significant at the $p < 0.01$ level 57

Chapter 1: Using a decision tree to create a historical multi-year land cover classification

Abstract

Land cover change impacts ecosystem function across the globe and the use of land cover data is vital in the detection of these changes over time. However, most available land cover products, such as the National Land Cover Dataset (NLCD), are produced infrequently. The most recent NLCD at the time of this research was produced in 2006, and may not adequately reflect the impact of land cover changes that have occurred since. Therefore, there is a need for the classification of historical imagery through replicable methods. While it is possible to collect field data coinciding with current or future Landsat acquisitions, it is impossible to collect data for previous years, thus very few studies have focused on the classification of historical imagery. Using a single year of field reference and multi-year aerial photography data we applied a simple decision tree classifier to accurately classify historic satellite images and produced maps of land cover to incorporate the effects of 2008 wildfires. Overall accuracy ranged from 76 to 90 percent and was assessed using conventional error matrices and a spatial representation of accuracy.

1. Introduction

Land cover change impacts ecosystem function across the globe (Lambin *et al.* 2001), and disturbance is a major driver of land cover change which creates heterogeneous landscapes (Turner 1989). Large infrequent disturbances, such as wildfires, are an essential component in many ecosystems but have the potential to produce unexpected changes (Turner

& Dale 1998), especially when coupled with other impacts such as a changing climate (Dale et al. 2001). Wildfires burn with varying degrees of severity which affects vegetation succession (Epting, Verbyla & Sorbel 2005), land management efforts (Patterson & Yool 1998), and the potential for increased erosion and flooding (Robichaud, Beyers & Neary 2000).

In California, wildfire is a common driver of land cover change (Sleeter *et al.* 2011) and in the Big Sur region of the central California coast, the majority of area burned is the result of large infrequent fires controlled primarily by extreme weather (Davis & Borchert 2006). These wildfires can significantly alter vegetation in watersheds that transport sediment and nutrients to the adjacent nearshore oceanic environment (Goodridge & Melack 2012) and large coastal wildfire events have been shown to impact marine mammals (Bowen *et al.* 2014; Venn-Watson *et al.* 2013). The sea otter (*Enhydra lutris*) is a key predator and indicator of nearshore ecosystem health. In southern California, the sea otter is listed as "Threatened" under the Endangered Species Act and is also protected under the Marine Mammal Protection Act and California state law due to reduced range and declining populations (U.S. Fish & Wildlife Service 2014). In addition to influences from oceanic and climate systems, changes in nearshore inputs from land cover change in adjacent terrestrial watersheds, such as toxins, sediment, nutrients, and pollutants, can have negative effects on ecosystem health and sea otter populations (Bodkin *et al.* 2002; Conrad *et al.* 2005; Johnson *et al.* 2009; Miller *et al.* 2010).

Land cover data are vital in the detection of change over time; these data are widely used in ecological applications. To accurately assess impacts to the nearshore environment and thus sea otters, land cover data must accurately reflect any change caused by recent

disturbance. The multi-resolution land characteristics consortium (MLCR) National Land Cover Dataset (NLCD) is a commonly used land cover dataset (Clark *et al.* 2003; Brewer *et al.* 2005; Eidenshink *et al.* 2007; Kolden & Abatzoglou 2012), however at the time of this study the most recent version of the NLCD was produced in 2006 (the 2011 NLCD was released in April 2014, at the completion of this research), and therefore does not reflect the impact of land cover changes that occurred in subsequent years. For example, in 2008 two large wildfires burned in the Big Sur region of the central California coast.

Detection of change in land cover requires multi-temporal assessments of land cover data. It has been common practice to analyze the difference between two image dates to document change. However, time series approaches are increasingly common (Cohen, Yang & Kennedy 2010; Kennedy, Yang & Cohen 2010). The Landsat multispectral data acquisition program, including Landsat Thematic Mapper (TM), Enhanced Thematic Mapper (ETM+), and Operational Land Imager (OLI), provides free, relatively high-resolution remotely sensed data from 1984 to present that are widely used to study land cover change and disturbance across at both regional and global scales.

One way to utilize such time series in understanding change is to classify multispectral imagery, and a variety of classification methods have been developed (Lu & Weng 2007). A decision tree (Breiman *et al.* 1984) uses recursive partitioning to divide a dataset into smaller subsets using decision rules that partitions the data into categorical classes (classification tree). For classification tree methods, the way in which the data are parsed can differ, though most decision methods produce relatively similar overall classification accuracy (Zambon *et al.* 2006). Decision tree classifiers are simple, computationally efficient, and transparent (Friedl & Brodley 1997). In addition, decision tree methods do not require statistical

assumptions regarding distributions, are able to process large nonparametric datasets, and use both continuous and categorical data (Zambon *et al.* 2006).

A challenge in creating a multi-temporal image classification is the collection of high-quality field data for training and validation. Although it is possible to collect field data coinciding with current or future Landsat acquisitions, it is impossible to conduct field sampling to collect data for land cover classification of previous years and incredibly difficult and cost-prohibitive to collect field data over large areas. In such cases, it is possible to use other sources of information to create reference data, such as higher resolution aerial photographs (Hubert-Moy, Cotonnec & Du 2001; Rogan *et al.* 2003; Lu & Weng 2007). Unfortunately, aerial photographs coinciding with satellite images are not always common, and therefore it becomes necessary to extrapolate the reference data over time and space (Xie, Sha & Bai 2010).

Despite the utility of multi-temporal land cover classification datasets, very few studies have focused on the classification of historical satellite imagery and most studies have focused on the use and classification of historic images for change detection. Xie, Sha & Bai (2010) classified historic Landsat TM images by relying on the temporal and spatial correlation of spectral features. Based on this demonstration of the spatial and temporal relationships between images over time, our goal was to develop a method for classifying a time series of Landsat data using a decision tree classifier developed with a single year of field observations. The success of the classification was then assessed using both the standard error matrix and a local representation of the error. Our objectives were to 1) create a parsimonious decision tree that accurately classified historic satellite images, and 2) produce maps of land cover from 2005 to 2012 for the Big Sur region that would incorporate the

effects of the 2008 fires. This land cover dataset will then be used as an input for modeling nonpoint source pollutant transport from the Big Sur coastal watersheds to the nearshore environment.

2. Methods

2.1. Study Area

The study area boundary is formed by 15 adjacent watersheds covering 87,638 ha in the northern portion of the Los Padres National Forest (Figure 1.1) and extends approximately 109 km along the Santa Lucia Range south of Monterey Bay. The Santa Lucia Range rises steeply from sea level to just below 1,800 m within a few km from the coast. The climate is Mediterranean with long, dry summers and warm, wet winters. Precipitation ranges from 65 cm annually near the coast to over 130 cm at higher elevations (Davis *et al.* 2010). Temperature generally increases from north to south and with distance from the coast, with coastal mean monthly temperature range from 10-13°C in winter to 16-18°C in summer (Davis & Borchert 2006). These weather and elevation gradients create a highly diverse ecosystem which has been identified as a global biodiversity "hotspot" (Myers *et al.* 2000). The study area consists of three ecological zones, each including a number of vegetation types. The coastal plains and foothills include grasslands, coastal sage scrub, chaparral, oak forests, and closed-cone pine forest. The lower montane zone includes a mixture of coastal sage scrub, chaparral and oak woodlands, and forests. The upper montane zone primarily contains mixed broadleaf evergreen and coniferous forests (Davis & Borchert 2006).

2.2. Satellite and Ancillary Data

To classify land cover through time, the Surface Reflectance Climate Data Record (CDR) produced by the Landsat Ecosystem Disturbance Adaptive Processing System (LEDAPS) was used. Surface Reflectance CDR processes Landsat scenes to at-surface reflectance using the second simulation of the satellite signal in the solar spectrum (6 S) (Masek & Vermote 2006). Seven CRD Landsat TM and two Landsat ETM+ scenes (Path 33/Row 34) were downloaded from EarthExplorer (http://earthexplorer.usgs.gov). Cloud free data were acquired for eight years from 2005 to 2012 within the months of July and August (Table 1.1). CRD Landsat data are Level-1 geometrically and terrain-corrected (Masek & Vermote 2006). Landsat ETM+ imagery after May 31, 2003 was affected by the failure of the Scan Line Corrector, which causes "stripes" of missing data (Chander, Markham & Helder 2009). Because of the relative clarity of the atmosphere and the static nature of vegetation during the summer months over the study site, missing data on June 19, 2012 were filled from the closest and most cloud-free image available from June 3, 2012.

The suite of potential predictor variables necessary for creating the classification tree included Landsat bands 1 through 5 and 7 from TM and ETM+ sensors (Table 1.2). We also calculated several indices such as the normalized differenced vegetation index (NDVI) (Rouse *et al.* 1974; Tucker 1979), normalized burn ratio (NBR) (Key & Benson 2006), and band ratios 4/3 and 7/4. NDVI has been used in decision tree classifiers to discriminate differences in vegetation from non-vegetation cover (Friedl & Brodley 1997).

NBR is calculated from atmospherically corrected at-sensor reflectance; NBR= (NIR – SWIR) /(NIR + SWIR), where NIR is the near infrared (Landsat TM band 4 (0.76 – 0.90 μm)/Landsat ETM+ band 4 (0.77 – 0.90 μm)) and SWIR is the shortwave infrared (Landsat

TM band 7(2.08 – 2.35µm)/Landsat ETM+ band 7(2.09-2.35µm)). Changes in NIR wavelengths indicate a change in green vegetation and biomass (Jensen 1983) whereas SWIR is sensitive to soil and plant moisture (Jensen 2007) as well as burnt vegetation, ash, and exposed soil (Smith *et al.* 2005). We also used tasseled cap transformations of greenness, wetness, and brightness (Crist 1985) because of their ability to discriminate differences in vegetation cover in a prior decision tree classification (Rogan *et al.* 2003). Incorporation of variables that utilize the spatial information has been shown to increase the accuracy of remote sensing classification (Wulder & Boots 1998; Atkinson & Lewis 2000; Ghimire, Rogan & Miller 2010). In general, smoothing methods can utilize the spatial dependence between neighboring pixels, where pixels in close proximity are more likely to be similar (Atkinson & Lewis 2000). To account for spatial dependence in the image due to both steep topographical gradients and the heterogeneous composition of plant communities, spectral bands of the TM and ETM+ sensors were filtered using a mean low-pass 3x3 filter (Jensen 2005).

To derive terrain variables, which have been shown to be useful in the classification of vegetation in southern California (Franklin, McCullough & Gray 2000), two 1-arc second USGS Nation Elevation Dataset (NED) tiles were mosaicked and processed to produce elevation, aspect, and slope.

2.3. Classification Scheme & Reference Data

Classification categories of forest, shrub, and grass were chosen as broad classes to subsume all vegetation community types in the study area. This coarse classification was used to match the required input land cover vegetation types for nonpoint source pollutant modeling (Chapter 2, this volume). Though both evergreen and mixed forest types are present

in the study area, the two classes were combined because of the small percentage of mixed forest and substantial confusion between the classes. Class definitions were based on those defined by the multi-resolution land characteristics consortium (MLCR) national land cover dataset (NLCD) (Homer *et al.* 2004) (Table 1.3).

Training and validation reference data were collected in the field for the 2012 classification tree in November 2012. Each sample point was collected to represent a pixel in one of the three cover classes. At each point, vegetation was assessed as a homogeneous pixel with a 30- by 30-m area. Due to rugged terrain and dense vegetation much of the study area is inaccessible, so the location of field sampling points was limited to areas accessible by roads and trails. To increase the pool of reference points and better cover the three vegetation classes, reference data were also sampled by photointerpretation of a 2012 National Agriculture Imagery Program (NAIP) aerial photograph on a dot grid over the study area. At each point, if an approximate 30- by 30-m area was a visually homogeneous patch it was recorded as one of the three classes. Photointerpretation yielded 360 reference points while field collection produced 219 reference points, for a total of 579 reference points (Table 1.4). Reference points were randomly divided into two subsets for training (75 percent) and validation (25 percent).

High resolution photos from NAIP were also available for 2005 and 2009 and were used to obtain validation data for these two years by photointerpretation from the same point grid. From this grid of points, 180 sites were identified for 2005 and 164 sites were identified for 2009. For the remaining years (2006 – 2008, 2010, 2011) persistent sites were used for validation. Persistent sites were defined as reference data collected from photointerpretation

that remained the same class in 2005 through 2009 and 2012 outside of the area of the two fires (i.e., outside of any known disturbance). This yielded 147 persistent sites (Table 1.4).

2.4. Classification Tree

Because field data were collected in 2012, it was considered as the "base" classification year. A base year classification tree was developed for 2012 with 23 spectral and ancillary variables and reference training data collected in the field and from high resolution aerial photographs from 2012. The Idrisi Classification Tree Analysis (CTA) module with the gain ratio algorithm option was used to develop the decision tree. Pruning levels of 1, 5, and 10 percent were all tested for their ability to produce the most parsimonious tree with the highest accuracy. The decision rules generated by the 2012 base tree were then applied to all preceding years of data (2011 – 2005), producing a classified map of land cover for each year.

2.5. Accuracy Assessment

We assessed classification accuracy using error matrices which provide overall accuracy of the map, per class errors of commission and omission, and the kappa statistic (Congalton 1991). A global estimate of overall accuracy (provided by the error matrix) may not be appropriate for all areas of the map, especially in sub-regions (Comber *et al.* 2012). Based on the methods from Comber *et al.* (2012), a geographically weighted logistic regression was also used to analyze how the classification accuracy varies across space. Because the presence or absence of a specific land cover class is binary, a logistic regression or logit model is used. Logistic models provide a probability ranging from 0 to 1 representing the correct prediction of a land cover class. When used in combination with geographically weighted regression

(GWR) (Fotheringham, Brundsdon & Charlton 2000) this allows for the local assessment of correctly classified and incorrectly classified land cover to vary over space. This assumption that relationships vary across space required the use of a moving kernel which only considers data within a specified window to obtain regression estimates. Data are weighed according to proximity to a point; data closer are weighted higher and, conversely, data further are weighted less (Fotheringham, Brundsdon & Charlton 2000). The results of the geographically weighted logistic regression provides the probability that the presence of the reference data is correctly identified by the classified data expressed as quartiles (Comber *et al.* 2012).

3. Results

3.1. Classification Tree

The classification tree for the 2012 data which was achieved with a 5 percent pruning level is shown in Figure 1.2. The decision tree analysis resulted in a simple tree which used only NDVI, Tasseled Cap, and the low pass filter of band 7 out of the 23 input variables, using NDVI twice. At the first node, NDVI was used to identify grass. This was the only terminal node at which grass was assigned, indicating the remainder of the classification tree nodes separated shrub from forest. At the second node the low pass mean filter of band 7 split forest into a terminal node. The second use of NDVI separated out a portion of the shrub points as having a lesser NDVI value and final node used tasseled cap greenness to separate the remaining shrub from forest.

3.2. Classification Accuracy

The 2012 classification produced a map with a 90 percent overall accuracy and 0.84 kappa (Table 1.4). The overall accuracies for all other years varied from 74 to 83 percent

with the highest accuracy in 2010 and the lowest in 2007 (Table 1.5). Kappa values ranged from the highest of 0.71 in 2010 and lowest of 0.56 in 2011 (Table 1.5). Overall and per class accuracies and kappa values for each year are reported in Table 1.5.

Accuracy associated with each class for 2012 is shown as minimum, median, maximum, and 1st and 3rd quartiles (Table 1.6). The inter-quartile range (IQR) shows the overall spatial variation in accuracy, the larger the value the greater the spatial variation (Comber *et al.* 2012). The class with the highest variability in 2012 was shrub cover (Figure 1.3). Quartiles for 2012 shrub are plotted as maps over the study area showing the spatial representation of the probabilities of correctly and incorrectly classified shrub cover from Table 1.5 (Figure 1.3). When the spatial map of probabilities are mapped along with reference data, the influence of the reference and classification points is apparent (Comber *et al.* 2012). For example, the accuracy map for 2012 shrub (Figure 1.3) demonstrates that areas where many points agree have a higher probability of correct prediction, whereas areas of less probability coincide with more frequent misclassifications. Areas where there are no reference data and are also shown as highly likely to be correctly predicted, as there is no error.

4. Discussion

The decision tree relied mainly on variables sensitive to vegetation characteristics. Ancillary variables were not chosen because, although the study area exhibits dramatic topographical gradients, the three land cover types are highly mosaicked across all topographic variables (Greenlee & Langenheim 1990; Davis & Borchert 2006). NDVI, sensitive to plant greenness and biomass, was used at the first node to identify grass which at the time was senesced, producing significantly lower NDVI values than shrub or forest cover.

The use of tasseled cap greenness (representing vegetation greenness) and NDVI were used to identify forest from shrub. The incorporation of spatial dependence by using a mean filter of band 7(sensitive to vegetation moisture) as was utilized to parse forest from shrub. The 2012 base classification was highly accurate, with an overall accuracy of 90 percent and a kappa of 0.84, where an accuracy of about 85 percent is argued as a minimum standard for overall accuracy (Wulder *et al.* 2006) and a kappa value of greater than 0.80 indicates high agreement between a classified map and reference data (Jensen 2005). However, once the 2012 decision tree was applied to the seven previous years of Landsat data, the overall accuracies fell ranging from 75 to 83 percent with kappa values ranging from 0.56 to 0.71. Low kappa values were a result of confusion among the classes, especially forest and shrub.

Because of its spectral dissimilarity from other classes, grass produced the highest accuracies, though some inaccuracies in grass can be attributed to areas where pasture land remains green from irrigation and the presence of nonnative species, and is classified as shrub. Shrub and forest classes consistently produced the lowest accuracies. Much of the vegetation in the study area is evergreen (both forest and shrub) and shrub cover in areas can be visually difficult to differentiate from forest, thus, the highest confusion was between the forest and shrub classes. In addition, patches of coast live oak forest grow extensively in grasslands and savannas (Davis & Borchert 2006) and can be difficult to differentiate from and are often classified as shrub.

In land cover classification with relatively high accuracy it may not be necessary to spatially map local accuracy. However, when a land cover classification results in low accuracy or has problematic classes of poor accuracy a spatial representation could be beneficial. Information from the maps of accuracy can be used to understand the causes of

variation (Foody 2005). Global measures of the 2012 overall classification accuracies was high, however the shrub cover class exhibited high variability as more points were both incorrectly classified into shrub from forest or out of shrub into forest or grass. Figure 1.3 shows a regional pattern of low probability of accuracy within the northern and southern portions of the study area. The southern region of the study area shows inaccuracies that could be a combination of lack of training points and incongruences between vegetation types and the classification scheme as three for the four reference point in the southern portion of the study area are misclassified. This type of spatially explicit accuracy could inform the appropriate choice of land cover data for an application (Comber 2013) or where specific regions are of a land cover map are not appropriate (Foody 2005). For large, difficult-to-access study sites this can indicate local problem areas in the classification method, and highlight regions of the study area where additional data is needed (Kyriakidis & Dungan 2001).

In general, higher accuracies can be achieved with the use of a simple classification scheme and a large number of training data (Congalton 1991). This was the case for the base 2012 year, however accuracy was not as high for the preceding years. This could be due to a number of reasons. First, the simplicity of the decision tree could have impacted the accuracy. To avoid over-fitting the decision tree with the 2012 data, we opted for the most parsimonious decision tree, however it is possible that the discrimination between forest and shrub could have benefited from a greater number of decision rules. Also, there is potential for error in the photointerpretation of validation points.

Though the classifications of seven historic Landsat images were less accurate compared to the 2012 base classification, overall the classification produced land cover maps

of moderate to high accuracy. We are confident that using these land cover maps will be sufficient in determining the effects of the 2008 wildfire on land cover and to the nearshore ecosystem.

5. Conclusion

Transitions in land cover and the disturbances that drive these transitions play a vital role in the function of ecosystems. Quantifying these changes relies on their inclusion into land cover datasets. Ample amounts of remotely sensed data provide many opportunities for the classification of land cover for monitoring land cover changes, however, lack of field data can make it difficult to use many classification methods. We present a relatively simple method for classifying historic remote sensing images in the absence of historic reference data given at least one year of quality reference data is available. Using this method, we successfully classified eight years of Landsat data with relative accuracy, including years that incorporated the impacts of wildfire. In Chapter 2, these land cover data will serve as the basis for a runoff model to quantify the impacts of wildfire and subsequent land cover changes to coastal watersheds and the nearshore environment.

Figures and Tables

Figure 1.1. Big Sur region of the central California coast, and the 2008 Basin Complex and Chalk fires.

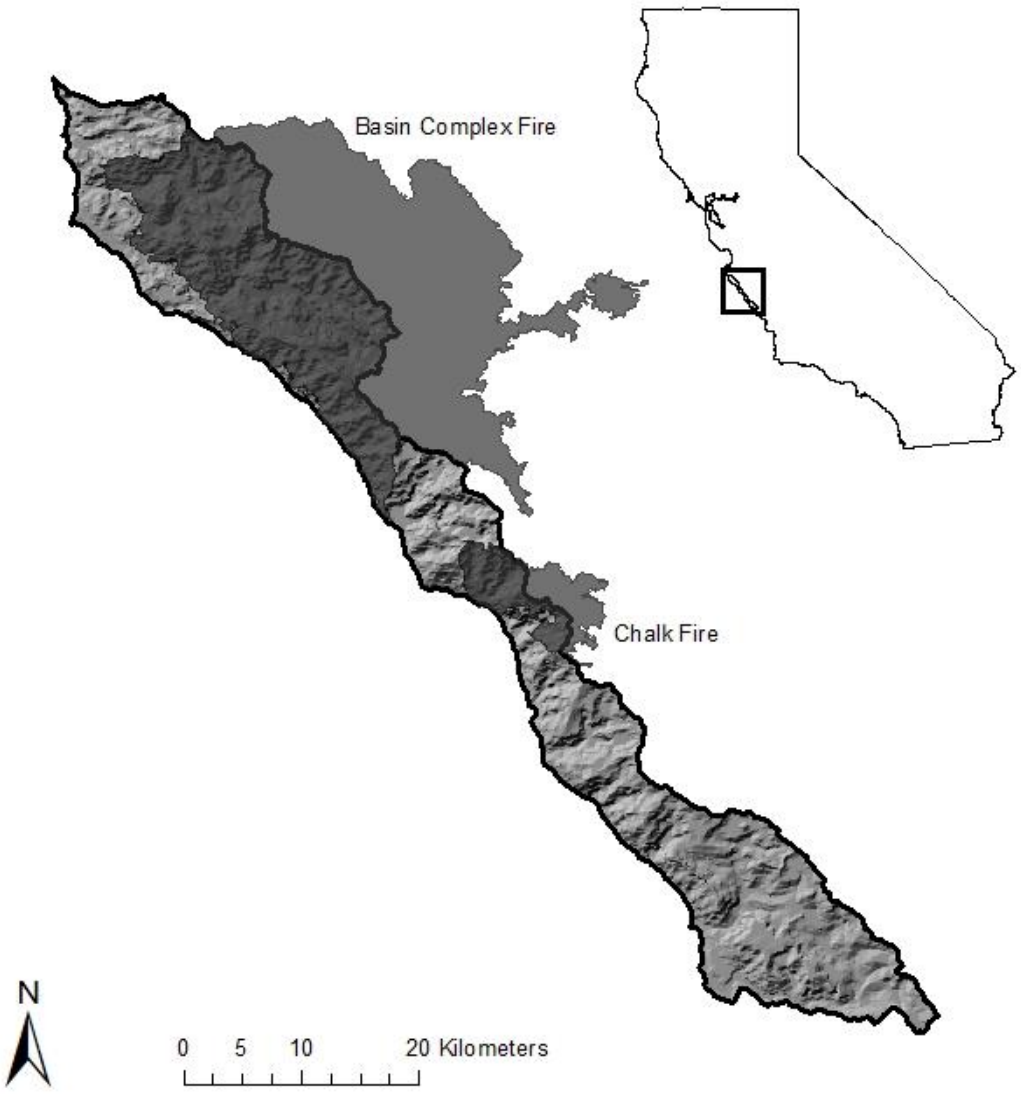

Figure 1.2. Classification tree for base year 2012, which was applied to all years.

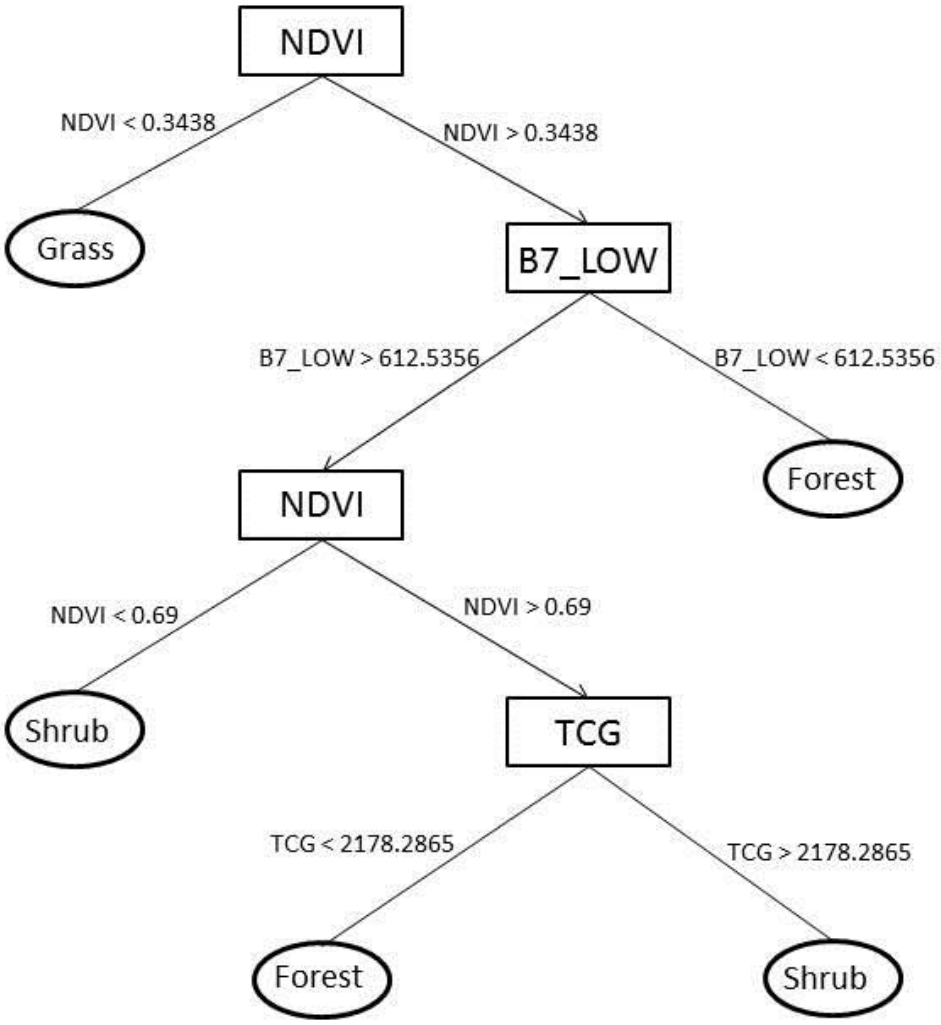

Figure 1.3. Maps of spatial distribution of accuracy for 2012 shrub cover. Values represent the probability of the presence of the correct class. Maps of agreement between reference data and classified map for 2012. Solid circles represent agreement in both data sets, unfilled circles represent shrub points incorrectly classified as forest or grass (omission error), and the crosses represent forest or shrub points incorrectly classified as shrub (commission error).

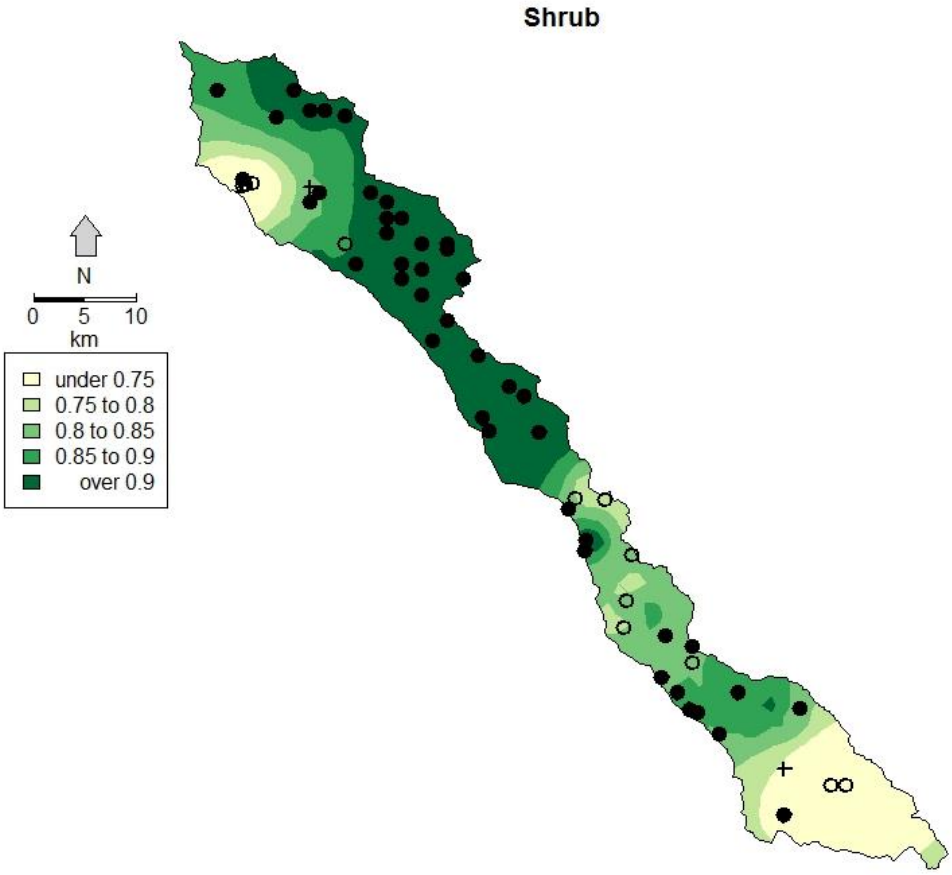

Table 1.1. Sensor name and date of acquisition for remotely sensed data.

Sensor	Year	Month/Day
Landsat TM	2005	8-Jul
	2006	11-Jul
	2007	14-Jul
	2008	1-Aug
	2009	19-Jul
	2010	23-Aug
	2011	25-Jul
Landsat ETM+	2012	19-Jul
	2012	3-Jul

Table 1.2. Spectral and ancillary input variables.

Variable	Description
Spectral	
Band 1 (B1)	0.45 - 0.52 µm TM, 0.45-0.515 µm ETM+
Band 2 (B2)	0.52 - 0.60 µm TM, 0.525-0.605 µm ETM+
Band 3 (B3)	0.63 - 0.69 µm TM,ETM+
Band 4 (B4)	0.76 - 0.90 µm TM, 0.75-0.90 µm ETM+
Band 5 (B5)	1.55 - 1.75 µm TM,ETM+
Band 7 (B7)	2.09 - 2.35 µm TM, 2.09-2.35 µm ETM+
Low Band 1	3x3 Mean Filter
Low Band 2	3x3 Mean Filter
Low Band 3	3x3 Mean Filter
Low Band 4	3x3 Mean Filter
Low Band 5	3x3 Mean Filter
Low Band 7	3x3 Mean Filter
4/3 ratio	B 4/ B 3
7/4 ratio	B 7 / B 4
NDVI	(B4 − B3)/(B4 + B3)
NBR	(B7 − B4)/(B7 + B4)
TCB	0.2043 ∗ B1 + 0.4158 ∗ B2 + 0.5524 ∗ B3 + 0.5741 ∗ B4 + 0.3124 ∗ B5 + 0.2303 ∗ B7
TCW	0.0315 ∗ B1 + 0.2021 ∗ B2 + 0.3102 ∗ B3 + 0.1594 ∗ B4 − 0.6806 ∗ B5–0.6109 ∗ B7
TCG	− 0.1603 ∗ B1 − 0.2819 ∗ B2 − 0.4934 ∗ B3 + 0.7940 ∗ B4 − 0.0002 ∗ B5 − 0.1446*B7
Ancillary	
Aspect	0 - 360
Slope	Degrees
Elevation	Meters

Table 1.3. Land cover classes based on the descriptions used for the National Land cover Dataset (NLCD).

Land-cover class	Class description
Forest	Areas dominated by trees generally greater than 5 m tall, and greater than 20 percent of total vegetation cover. Includes both evergreen forest where canopy is never without green and mixed forest where deciduous nor evergreen species are greater than 75 % of the total tree cover
Shrub	Areas dominated by shrubs less than 5 m tall with shrub canopy typically greater than 20% of total vegetation. Includes true shrubs, young trees in early successional stage, or trees stunted from environmental conditions
Grass	Areas dominated by grammaniod or herbaceous vegetation, generally greater than 80 % of the total vegetation. Includes grazing

Table 1.4. References data obtained for classification. NAIP sources were photointerpreted from a point grid over the study area. Persistent sites consist of photointerpreted sites that remained constant from 2005 through 2009 and 2012. 2012 sites were divided into training (75 percent) and validation (25 percent), for all other years, sites were used for validation.

Year	Data source	Number of sites	Purpose
2012	Field	219	Training & Validataion
	NAIP	360	Training & Validataion
2011	Persistent sites	147	Validation
2010	Persistent sites	147	Validation
2009	NAIP	164	Validation
2008	Persistent sites	147	Validation
2007	Persistent sites	174	Validation
2006	Persistent sites	147	Validation
2005	NAIP	180	Validation

Table 1.5. Classification error matrices for each year.

		Reference				
Year	Classified	Forest	Shrub	Grass	Total	Commission Error
2005	Forest	70	18	1	89	0.21
	Shrub	15	48	1	64	0.25
	Grass	0	9	18	27	0.33
	Total	85	75	20	0.76	Overall
	Omission Error	0.18	0.36	0.10	0.59	Kappa
	Classified	Forest	Shrub	Grass	Total	Commission Error
2006	Forest	58	14	1	73	0.21
	Shrub	9	39	8	56	0.30
	Grass	0	3	15	18	0.17
	Total	67	56	24	0.76	Overall
	Omission Error	0.13	0.30	0.38	0.61	Kappa
	Classified	Forest	Shrub	Grass	Total	Commission Error
2007	Forest	47	24	2	73	0.36
	Shrub	3	46	7	56	0.18
	Grass	0	1	17	18	0.06
	Total	50	71	26	0.75	Overall
	Omission Error	0.06	0.35	0.35	0.60	Kappa
	Classified	Forest	Shrub	Grass	Total	Comission Error
2008	Forest	49	24	0	73	0.33
	Shrub	3	49	4	56	0.13
	Grass	0	1	17	18	0.06
	Total	52	74	21	0.78	Overall
	Omission Error	0.06	0.34	0.19	0.65	Kappa

		Reference				
Year	Classified	Forest	Shrub	Grass	Total	Commission Error
2009	Forest	56	23	0	79	0.29
	Shrub	7	49	4	60	0.18
	Grass	1	4	20	25	0.20
	Total	64	76	24	0.76	Overall
	Omission Error	0.13	0.36	0.17	0.62	Kappa
	Classified	Forest	Shrub	Grass	Total	Commission Error
2010	Forest	63	10	0	73	0.14
	Shrub	11	44	1	56	0.21
	Grass	0	3	15	18	0.17
	Total	74	57	16	0.83	Overall
	Omission Error	0.15	0.23	0.06	0.71	Kappa
	Classified	Forest	Shrub	Grass	Total	Commission Error
2011	Forest	59	14	0	73	0.19
	Shrub	16	39	1	56	0.30
	Grass	0	7	11	18	0.39
	Total	75	60	12	0.74	Overall
	Omission Error	0.21	0.35	0.08	0.56	Kappa
	Classified	Forest	Shrub	Grass	Total	Commission Error
2012	Forest	35	13	0	48	0.27
	Shrub	1	44	1	46	0.04
	Grass	0	0	50	50	0.00
	Total	36	57	51	0.90	Overall
	Omission Error	0.03	0.23	0.02	0.84	Kappa

Table 1.6. Quartiles for geographically weighted logistic regression representing probability of the classification correctly predicting the reference data. Interquartile range (IQR) represents the variability in probability.

Year	Class	Min.	1st Qu.	Median	Mean	3rd Qu.	Max.	IQR
2012	Forest	0.84	0.88	0.91	0.91	0.93	1.00	0.045
	Shrub	0.60	0.85	0.90	0.89	0.93	1.00	0.082
	Grass	0.91	0.99	1.00	0.99	1.00	1.00	0.008

References

Atkinson, P. & Lewis, P. (2000) Geostatistical classification for remote sensing: an introduction. *Computers & Geosciences*, **26**, 361–371.

Bodkin, J., Ballachey, B., Dean, T., Fukuyama, A., Jewett, S., McDonald, L., Monson, D., O'Clari, C. & VanBlaricom, G. (2002) Sea otter population status and the process of recovery from the 1989 "Exxon Valdez"oil spill. *Marine Ecology Progress Series*, **241**, 237–253.

Bowen, L., Miles, A., Kolden, C., Saarinen, J., Murray, M. & Tinker, T. (2014) Effects of wildfire on sea otter (Enhydra lutris) immune function. *Marine Mammal Science*.

Breiman, L., Freedman, J., Olshen, R. & Stone, C. (1984) *Classification and Regression Trees*. Wadsworth, Belmont, Ca.

Brewer, C.K., Winne, J.C., Redmond, R.L., Opitz, D.W. & Mangrich, M. V. (2005) Classifying and Mapping Wildfire Severity : A Comparison of Methods. *Photogrammetric Engineering & Remote Sensing*, **71**, 1311–1320.

Chander, G., Markham, B.L. & Helder, D.L. (2009) Summary of current radiometric calibration coefficients for Landsat MSS, TM, ETM+, and EO-1 ALI sensors. *Remote Sensing of Environment*, **113**, 893–903.

Clark, J., Parsons, A., Zajkowski, T. & Lannom, K. (2003) *Remote Sensing Imagery Support for Burned Area Emergency Response Teams on 2003 Southern California Wildfires*. Salt Lake City, Utah.

Cohen, W.B., Yang, Z. & Kennedy, R. (2010) Detecting trends in forest disturbance and recovery using yearly Landsat time series: 2. TimeSync — Tools for calibration and validation. *Remote Sensing of Environment*, **114**, 2911–2924.

Comber, A. (2013) Geographically weighted methods for estimating local surfaces of overall, user and producer accuracies. *Remote Sensing Letters*, 1–9.

Comber, A., Fisher, P., Brunsdon, C. & Khmag, A. (2012) Spatial analysis of remote sensing image classification accuracy. *Remote Sensing of Environment*, **127**, 237–246.

Congalton, R.G.R. (1991) A review of assessing the accuracy of classifications of remotely sensed data. *Remote Sensing of Environment*, **46**, 35–46.

Conrad, P.A., Miller, M.., Kreuder, C., James, E.R., Mazet, J., Dabritz, H., Jessup, D.A., Gulland, F. & Grigg, M.E. (2005) Transmission of Toxoplasma: clues from the study of sea otters as sentinels of Toxoplasma gondii flow into the marine environment. *International journal for parasitology*, **35**, 1155–68.

Crist, E.P. (1985) SHORT COMMUNICATION A TM Tasseled Cap Equivalent Transformation for Reflectance Factor Data. *Remote Sensing of Environment*, **306**, 301–306.

Dale, V.H., Joyce, L. a., Mcnulty, S., Neilson, R.P., Ayres, M.P., Flannigan, M.D., Hanson, P.J., Irland, L.C., Lugo, A.E., Peterson, C.J., Simberloff, D., Swanson, F.J., Stocks, B.J. & Michael Wotton, B. (2001) Climate Change and Forest Disturbances. *BioScience*, **51**, 723.

Davis, F.W. & Borchert, M.I. (2006) Central Coast Bioregion. *Fire in Califorina's Ecosystems* (eds N.G. Sugihara, J.W. Wagtendonk, K.E. Shaffer, J. Fites-Kaufman & A.E. Thode), p. 596. University of California Press.

Davis, F.W., Borchert, M., Meentemeyer, R.K., Flint, A. & Rizzo, D.M. (2010) Pre-impact forest composition and ongoing tree mortality associated with sudden oak death in the Big Sur region; California. *Forest Ecology and Management*, **259**, 2342–2354.

Eidenshink, J., Schwind, B., Brewer, K., Zhu, Z., Quayle, B., Howard, S. & Falls, S. (2007) A project for monitoring trends in burn severity. *Fire Ecology*, **3**, 3–21.

Epting, J., Verbyla, D. & Sorbel, B. (2005) Evaluation of remotely sensed indices for assessing burn severity in interior Alaska using Landsat TM and ETM+. *Remote Sensing of Environment*, **96**, 328–339.

Foody, G.M. (2005) Local characterization of thematic classification accuracy through spatially constrained confusion matrices. *International Journal of Remote Sensing*, **26**, 1217–1228.

Fotheringham, S.A., Brundsdon, C. & Charlton, M. (2000) *Quantitative Geography*. SAGE, London.

Franklin, J., McCullough, P. & Gray, C. (2000) Terrain variables used for predictive mapping of vegetation communities in Southern California. *Terrain analysis: principles and Applications* (eds J.P. Wilson & J.C. Gallant), pp. 331–353. John Wiley & Sons, Inc.

Friedl, M. & Brodley, C. (1997) Decision tree classification of land cover from remotely sensed data. *Remote sensing of environment*, **61**, 399–409.

Ghimire, B., Rogan, J. & Miller, J. (2010) Contextual land-cover classification: incorporating spatial dependence in land-cover classification models using random forests and the Getis statistic. *Remote Sensing Letters*, **1**, 45–54.

Goodridge, B.M. & Melack, J.M. (2012) Land use control of stream nitrate concentrations in mountainous coastal California watersheds. *Journal of Geophysical Research: Biogeosciences*, **117**, 1–17.

Greenlee, J. & Langenheim, J. (1990) Historic fire regimes and their relation to vegetation patterns in the Monterey Bay area of California. *American Midland Naturalist*, **124**, 239–253.

Homer, C., Huang, C., Yang, L., Wylie, B. & Coan, M. (2004) Development of a 2001 national landcover database for the United States. *Photogrammetric Engineering & Remote Sensing*, **70**, 829–840.

Hubert-Moy, L., Cotonnec, A. & Du, L. Le. (2001) A comparison of parametric classification procedures of remotely sensed data applied on different landscape units. *Remote Sensing of Environment*, **75**, 174–187.

Jensen, J.R. (1983) Review Article: Biophysical Remote Sensing. *Annals of the Association of American Geographers*, **73**, 111–132.

Jensen, J.R. (2005) *Introductory Digital Image Processing*, Thrid Edit. Prentice Hall.

Jensen, J.R. (2007) *Remote Sensing of the Environment An Earth Resource Perspective*, 2nd ed. Pearson Prentice Hall.

Johnson, C.K., Tinker, M.T., Estes, J. a, Conrad, P. a, Staedler, M., Miller, M. a, Jessup, D. a & Mazet, J. a K. (2009) Prey choice and habitat use drive sea otter pathogen exposure in a resource-limited coastal system. *Proceedings of the National Academy of Sciences of the United States of America*, **106**, 2242–7.

Kennedy, R.E., Yang, Z. & Cohen, W.B. (2010) Detecting trends in forest disturbance and recovery using yearly Landsat time series: 1. LandTrendr — Temporal segmentation algorithms. *Remote Sensing of Environment*, **114**, 2897–2910.

Key, C.H. & Benson, N.C. (2006) Landscape Assessment (LA) Sampling and Analysis Methods. *USDA Forest Service Gen. Tech Rep. RMRS-GTR-164-CD*, 55.

Kolden, C. a. & Abatzoglou, J.T. (2012) Wildfire Consumption and Interannual Impacts by Land Cover in Alaskan Boreal Forest. *Fire Ecology*, **7**, 98–114.

Kyriakidis, P. & Dungan, J. (2001) A geostatistical approach for mapping thematic classification accuracy and evaluating the impact of inaccurate spatial data on ecological model predictions. *Environmental and ecological statistics*, 311–330.

Lambin, E.F., Turner, B.L., Geist, H.J., Agbola, S.B., Angelsen, A., Bruce, J.W., Coomes, O.T., Dirzo, R., Fischer, G., Folke, C., George, P.S., Homewood, K., Imbernon, J., Leemans, R., Li, X., Moran, E.F., Mortimore, M., Ramakrishnan, P.S., Richards, J.F., Skånes, H., Steffen, W., Stone, G.D., Svedin, U., Veldkamp, T. a., Vogel, C. & Xu, J. (2001) The causes of land-use and land-cover change: moving beyond the myths. *Global Environmental Change*, **11**, 261–269.

Lu, D. & Weng, Q. (2007) A survey of image classification methods and techniques for improving classification performance. *International Journal of Remote Sensing*, **28**, 823–870.

Masek, J. & Vermote, E. (2006) A Landsat surface reflectance dataset for North America, 1990-2000. *IEEE Geoscience and Remote Sensing Letters*, **3**, 68–72.

Miller, M. a, Kudela, R.M., Mekebri, A., Crane, D., Oates, S.C., Tinker, M.T., Staedler, M., Miller, W. a, Toy-Choutka, S., Dominik, C., Hardin, D., Langlois, G., Murray, M., Ward, K. & Jessup, D. a. (2010) Evidence for a novel marine harmful algal bloom: cyanotoxin (microcystin) transfer from land to sea otters. *PloS one*, **5**.

Myers, N., Mittermeier, R. a, Mittermeier, C.G., da Fonseca, G. a & Kent, J. (2000) Biodiversity hotspots for conservation priorities. *Nature*, **403**, 853–8.

Patterson, M. & Yool, S. (1998) Mapping fire-induced vegetation mortality using Landsat Thematic Mapper data: A comparison of linear transformation techniques. *Remote Sensing of Environment*, **65**, 132–142.

Robichaud, P., Beyers, J. & Neary, D. (2000) Evaluating the effectiveness of postfire rehabilitation treatments. *USDA Forest Service Rocky Mountain Research Station General Technical Report RMSR-GTR-63*, 89.

Rogan, J., Miller, J., Stow, D. & Franklin, J. (2003) Land-cover change monitoring with classification trees using Landsat TM and ancillary data. *Photogrammetric Engineering & Remote Sensing*, **69**, 793–804.

Rouse, J.W., Haas, J.A., Schell, J.A., Deering, D.W. & Harlan, J.C. (1974) *Monitoring the Vernal Advancement of Retrogradation of Natural Vegetation*. Greenbelt, MD.

Sleeter, B.M., Wilson, T.S., Soulard, C.E. & Liu, J. (2011) Estimation of late twentieth century land-cover change in California. *Environmental monitoring and assessment*, **173**, 251–66.

Smith, A.M.S., Wooster, M.J., Drake, N. a., Dipotso, F.M., Falkowski, M.J. & Hudak, A.T. (2005) Testing the potential of multi-spectral remote sensing for retrospectively estimating fire severity in African Savannahs. *Remote Sensing of Environment*, **97**, 92–115.

Tucker, C.J. (1979) Red and photographic infrared linear combinations for monitoring vegetation. *Remote Sensing of Environment*, **8**, 127–150.

Turner, M. (1989) Landscape ecology: the effect of pattern on process. *Annual review of ecology and systematics*, **20**, 171–197.

Turner, M. & Dale, V. (1998) Comparing large, infrequent disturbances: what have we learned? *Ecosystems*, **1**, 493–496.

U.S. Fish & Wildlife Service. (2014) Southern Sea Otter Information, http://www.fws.gov/Ventura/species_information/so_sea_otter/index.html. Accessed February 2014.

Venn-Watson, S., Smith, C.R., Jensen, E.D. & Rowles, T. (2013) Assessing the potential health impacts of the 2003 and 2007 firestorms on bottlenose dolphins (Trusiops trucatus) in San Diego. *Inhalation toxicology*, **29**, 481–491.

Wulder, M. & Boots, B. (1998) Local spatial autocorrelation characteristics of remotely sensed imagery assessed with the Getis statistic. *International Journal of Remote Sensing*, **19**, 2223–2231.

Wulder, M., Franklin, S., White, J., Linke, J. & Magnussen, S. (2006) An accuracy assessment framework for large-area land cover classification products derived from medium-resolution satellite data. *International Journal of Remote Sensing*, **27**, 663–683.

Xie, Y., Sha, Z. & Bai, Y. (2010) Classifying historical remotely sensed imagery using a tempo-spatial feature evolution (T-SFE) model. *ISPRS Journal of Photogrammetry and Remote Sensing*, **65**, 182–190.

Zambon, M., Lawrence, R., Bunn, A. & Powell, S. (2006) Effect of alternative splitting rules on image processing using classification tree analysis. *Photogrammetric Engineering & Remote Sensing*, **72**, 25–30.

Chapter 2: Impacts of wildfire on coastal watersheds and the nearshore environment in Big Sur, California

Abstract

In the Mediterranean ecosystems of coastal California, wildfire is a common disturbance that can significantly alter vegetation in watersheds that transport sediment and nutrients to the adjacent nearshore oceanic environment. We assess the impact of two wildfires that burned in 2008 on land cover and the nearshore environment along the Big Sur coast in central California. Nonpoint source pollutants were modeled using a GIS-based empirical deterministic model utilizing multi-year land cover that incorporates wildfire effects to quantify export to the nearshore environment resulting from the fire effects. Results indicate post-fire concentration increases in phosphorus by 161 percent, sediments by 350 percent and total suspended solids (TSS) by 53 percent above pre-fire years. Result also link wildfire severity to the specific land cover changes that subsequently increase exports of pollutants and sediment to the nearshore environment. The approach used is not only replicable across other watersheds but also provides a framework for land management of wildfire, including suppression, thinning, and post-fire rehabilitation and other activities that change land cover at a landscape scale for assessing potential negative impacts to the nearshore environment in coastal basins.

1. Introduction

Wildfire is an integral natural disturbance in many ecosystems. Anthropogenic climate change, however, is predicted to alter fire characteristics through the century (Westerling *et*

al. 2006; Littell *et al.* 2009), creating disturbance patterns that may alter ecosystems in unprecedented ways. Wildfire is a common disturbance in Mediterranean ecosystems of coastal California watersheds draining into the Pacific ocean (Keeley & Zedler 2009). These large coastal wildfire events have been shown to impact marine mammal immune response (Bowen *et al.* 2014; Venn-Watson *et al.* 2013). As a key marine mammal predator, the sea otter (*Enhydra lutris*), is an indicator of nearshore ecosystem health. In southern California, the sea otter is listed as "Threatened" under the Endangered Species Act and protected under the Marine Mammal Protection Act (U.S. Fish & Wildlife Service 2014). Despite protection, the California sea otter population is recovering at a lower-than-expected rate, leading to queries seeking to identify factors impeding population growth rate (Johnson *et al.* 2009). Inputs to the sea otter's nearshore habitat from terrestrial watersheds, such as toxins, nutrients, and pollutants, have been shown to negatively affect sea otter health (Conrad *et al.* 2005; Johnson *et al.* 2009; Miller *et al.* 2010), but prior studies have focused primarily on pathogens (Johnson *et al.* 2009) or large, anthropogenic spill events like the Exxon Valdez oil spill of 1989 (Bodkin *et al.* 2002).

Wildfire significantly alters vegetation in watersheds that supply sediment and nutrients to the adjacent nearshore oceanic environment (Goodridge & Melack 2012). In altering the condition of soil and vegetation, fire effects can drastically alter the hydrologic response of a watershed by affecting infiltration and transport of nutrients and metals (Stein *et al.* 2012) and increasing erosion and sediment yields (Warrick *et al.* 2012; Moody *et al.* 2013). The loss of vegetation and duff and litter layers reduces interception thereby altering infiltration of rainfall (Baker 1990). In addition, severe fire often cause hydrophobic soils (Shakesby & Doerr 2006) especially in chaparral ecosystems (Warrick *et al.* 2012) further

increasing runoff. Wildfire has been shown to increase the amount of phosphorus and nitrogen in streams (Spencer & Hauer 1991; Coombs & Melack 2013), even many years after a wildfire (Hauer & Spencer 1998), as well as sediment loads (Warrick *et al.* 2012). In coastal California watersheds these post-fire increases in runoff of sediment and nutrients have been measured within streams (Warrick *et al.* 2012; Stein *et al.* 2012), suggesting that large wildfires might also impact the nearshore environment as these nutrients and sediments then drain into the ocean. The effects of wildfire on the increasing transport of sediment and nutrients have been shown to adversely affect freshwater aquatic ecosystems (Gresswell 1999; Spencer, Gabel & Hauer 2003), however, the effect of these increases in marine ecosystems has not been well documented.

The specific effects of fire on the nearshore ecosystem are difficult to delineate from *in-situ* stream sampling, as wildfires often burn only portions of watersheds and burn with varying severity across watersheds. Additionally, the results from studies collecting *in-situ* measurements are not transferable to other fires or to watersheds across time and space due to the spatial variability of burn severity across the landscape (Shakesby & Doerr 2006). To our knowledge, no prior studies have attempted to model the spatially explicit impacts of a wildland fire event on runoff into the nearshore environment using a replicable, watershed-scale approach.

To quantify spatially explicit impacts of wildfire on nonpoint source pollutants, an approach must utilize model inputs that reflect the spatially and temporally variable wildfire effects on relevant inputs. The primary input affected by wildfire at landscape scales is land cover, which is often classified from remotely sensed data and combines both vegetation and human development. Commonly available land cover datasets such as the National Land

Cover Dataset (NLCD) (U.S. Geological Survey 2014) are widely used, but can be limiting because they are produced at infrequent intervals due to the challenges of acquiring adequate remotely sensed data and the intense effort required to produce continental-scale classifications. For example, the most recent NLCD data when this research was conducted was produced in 2006 (the 2011 NLCD was released in April 2014) and as a result does not account for subsequent years of land cover transition, including two large wildfires that burned on the Big Sur coast in 2008. Incorporating these land cover disturbances is essential to accurately accounting changes in sources of nonpoint sources of nutrients and sediments.

Prediction of post-fire effects has focused on runoff and erosion rates and relied on a variety of physically and empirically based models, spatially distributed models, and professional judgment (Larsen & MacDonald 2007). Commonly used post-fire runoff models such as ERMIT (Robichaud *et al.* 2007), RUSLE (Renard & Foster 1991), and Disturbed WEPP (Elliot & Hall 2010) include land cover as an input, but are not not spatially explicit (*but see* Renschler 2003). Nutrient outputs such as phosphorus and nitrogen are also not commonly modeled. The use of these models produces a wide range of runoff estimates, making comparisons difficult (Robichaud, Beyers & Neary 2000). In addition, few have been validated in post-fire environments (Larsen & MacDonald 2007). Among models that have been tested for post-fire erosion, result have demonstrated that the amount of vegetation cover post-fire has a strong impact on erosion rates (De Dios Benavides-Solorio & MacDonald 2005). Following wildfire, vegetation communities continue along established succession pathways or undergo type conversions from one community to another along alternative pathways (Fites-Kaufman, Bradley & Merrill 2006). The severity of a fire, often described as ‘burn severity’, or the magnitude of change in the post fire environment (Key & Benson

2006), impacts vegetation succession (Epting, Verbyla & Sorbel 2005), vegetation composition and structure (Lentile 2005; Keeley, Brennan & Pfaff 2008) and therefore the potential for increased erosion and flooding (Robichaud, Beyers & Neary 2000). Understanding burn severity across landscapes and the resulting changes within these landscapes is especially important when considering effects occurring in coupled ecosystems like the nearshore environment and its adjacent terrestrial watersheds. Much research has been focused on characterizing burn severity through remotely sensed data (Key & Benson 2004; van Wagtendonk et al. 2004; Cocke et al. 2005; Miller & Thode 2007; Rogan & Franklin 2001; Walz et al. 2007) and looking at changes and trends in burn severity (Miller et al. 2008, Miller and Safford 2013). While several longitudinal studies have monitored vegetation succession after wildfire at the plot scale (Keeley & Zedler 1978; Greenlee & Langenheim 1990; Callaway & Davis 1993; Santana, Baeza & Maestre 2012), few studies have looked at relationships between burn severity and vegetation at landscape scales. These have mostly focused on characterizing pre-fire vegetation contributions to post-fire severity (Miller & Thode 2007; Dillon *et al.* 2011; Kolden & Abatzoglou 2012) rather than linking severity to post-fire transitions, in part due to the relatively recent development of representative spectral indices that allow burn severity to be mapped.

Quantifying the relative impacts of wildfire on land cover change and subsequent runoff is critical to understanding how terrestrial disturbance and change can impact threatened species in the nearshore environment. While most studies surrounding the limited growth of the sea otter population in central California have focused on anthropogenic inputs particularly in Monterey Bay (Conrad *et al.* 2005; Dowd, Press & Huertos 2008; Johnson *et al.* 2009), the Big Sur population of sea otters is comparatively isolated and protected from

anthropogenic inputs, but still limited in terms of population growth. We hypothesize that large wildfires have similar detrimental effects as anthropogenic inputs to the nearshore environment due to altered land cover and subsequent increases in modeled nonpoint source pollutants that the watersheds with the highest burn severity have the greatest increases in runoff following wildfire. Here, our goal was to assess the impact of two wildfires that burned in 2008 on land cover and to determine the sensitivity of nonpoint source pollutants into the nearshore environment to changes in land cover along the Big Sur coast in central California. Our objectives were: 1) to characterize the effect of burn severity on land cover within the study area, 2) to model nonpoint source pollutants utilizing a multi-year land cover time series that incorporates wildfire effects, and 3) to quantify the changes in modeled nonpoint source pollutants to the nearshore environment resulting from the fire effects.

2. Methods

2.1. Study Area

The study area is located on the central California coast and extends approximately 109 km along the Santa Lucia Range south of Monterey Bay (Figure 2.1). The boundary is formed by twelve adjacent watersheds covering 87,638 ha and draining a portion of the Santa Lucia Range in the northern portion of the Los Padres National Forest. All but one of the watersheds drain west-facing slopes from coast to ridgeline. The Santa Lucia Range rises steeply from sea level to just below 1,800 m within a few km from the coast. The area has a Mediterranean climate with long dry summers and wet winters with a fire season typically lasting from June to November (Greenlee & Langenheim 1990). Precipitation is dependent on elevation ranging from 65 cm near the coast to over 130 cm at ridge top (Davis *et al.* 2010).

Average temperature generally increases from north to south and with distance from the coast. Coastal mean monthly temperature ranges from 10°C-13°C in winter to 16°C-18°C in summer (Davis & Borchert 2006). These weather and elevation gradients create a highly diverse ecosystem which has been identified as a global biodiversity "hotspot" (Myers *et al.* 2000). From the coast inward, there are three ecological zones within the study area, each including a number of vegetation types. The coastal plains and foothills zone includes grasslands, coastal sage scrub, chaparral, oak forests, and closed cone pine forest. The lower montane zone includes a mixture of coastal sage scrub, chaparral and oak woodlands and forests. The upper montane zone primarily contains mixed broadleaf evergreen and coniferous forests (Davis & Borchert 2006).

In the Big Sur region, the majority of area burned is from large infrequent fires controlled primarily by extreme weather with return intervals estimated to be 75 years on average (Davis & Borchert 2006). Prior to 2008, the most recent fires to burn through portions of the study area were the 1977 Marble Cone Fire (72,500 ha) and the 1999 Kirk Complex (35,100 ha). In 2008 two large fires, the Basin Complex and the Chalk Fires, burned approximately 33,038 ha, or 42 percent of the study area. The Basin Complex Fire burned from June 21 to July 27, 2008 and the Chalk Fire burned from September 27 to October 30. Both fires were contained before the onset of the rainy season, which is from November through March (Davis & Borchert 2006).

2.2. Fire Effects

To characterize the effects of the 2008 wildfires on land cover, classifications of land cover and burn severity derived from remotely sensed data were explored. A land cover dataset for each year from 2005 to 2012 was developed in order to capture the effects of the

2008 fires (Chapter 1, this volume). Land cover was classified into one of three types: forest, shrub, or grass. These three classes are the dominant vegetation types across the study accounting for 97 percent of all land cover. Because bare ground was such a small percentage of the study area (< 0.01 percent) it was not specifically classified and because of spectral similarity to senesced grass was classified as grass. Due to the date of image acquisition (August 1, 2008) and the timing of the early summer Basin Complex Fire (June) and the late ignition of the Chalk Fire (September), fire effects from the Basin Complex are recorded in the 2008 land cover data approximately one month after the fire burned while fire effects from the Chalk Fire are recorded approximately one year post fire in the 2009 land cover data. Land cover changes for each class were quantified by plotting the change in percent cover over time between burned and unburned areas. Error was accounted for using error matrices to provide a measure of overall and per class accuracy (Chapter1, this volume). The overall classification accuracy ranged from 75 to 90 percent for the eight years of land cover maps produced. Individual class accuracies were quantified using the commission error which indicated the probability that a pixel on the classified land cover map represents the same category if you were standing in the field (Congalton 1991). The commission error for each land cover class was then averaged over all years.

Landscape-scale burn severity is commonly represented with a spectral index called the differenced Normalized Burn Ratio (dNBR) (Key & Benson 2006). The NBR is calculated from atmospherically-corrected at-surface reflectance; NBR= (NIR – SWIR) / (NIR + SWIR). The differenced equation, dNBR, is produced by subtracting the post-fire NBR image from the pre-fire NBR, creating an index representing a magnitude of change (Key & Benson 2006). Changes in NIR wavelengths indicate a change in green vegetation

and biomass (Jensen 1983) whereas SWIR wavelengths are documented to have sensitivity to soil and plant moisture (Jensen 2007) as well as burnt vegetation, ash, and exposed soil (Smith *et al.* 2005).

Four metrics were calculated to represent the effects of fire for each basin (Table 2.1). First, percent high burn severity (HS) was calculated from the dNBR using a threshold of 367, which was identified by Miller & Thode (2007) as being correlated to field measures in a variety of vegetation types in the Sierra Nevada having high to complete vegetation morality. Second, the Severity Metric (SM; Lutz *et al.* 2011) was calculated based on the dNBR. Lutz et al. (2011) developed the Severity Metric to represent burn severity continuously. Grouping burn severity or using a threshold to determine discrete classes is necessary as a means to communicate the effects of fire and in accounting for differences in scale and diverse methods used to measure burn severity for different fires (Miller & Thode 2007). However, separating burn severity into discrete categories can be problematic when classes differ between studies (Miller & Thode 2007), and information can be lost in the process (Lutz *et al.* 2011). The Severity Metric is computed as one minus the area under the cumulative distribution for a specified range of dNBR (Lutz *et al.* 2011).

Finally, two transitions in land cover were calculated: 1) the percent of pixels that transitioned from forest to shrub or from forest to grass (characterized as ‘Forest Loss’) and 2) the percent of pixels that transitioned from shrub to grass (‘Shrub Loss’). These two vegetation transition metrics were calculated for two temporal periods for each watershed, from 2006 to 2008 and from 2006 to 2009, to capture the effects of both fires. For consistency, 2006 was chosen as the pre-fire year instead of 2007 because the study area received only 50 percent of average precipitation in 2007 (California Department of Water

Resources 2010), and the subsequent drought stress effects on vegetation had a noticeable effect of reducing the accuracy of the 2007 land cover classification (Chapter 1, this volume). Because not all burned basins were 100 percent burned, the majority of remaining pixels not categorized as Forest Loss or Shrub Loss did not transition and remained the same between the years. The rest of pixels transitions (< 2 percent) were considered to be background noise as changes in land cover classes can be a result of classification accuracy and not an ecological process (Foody 2002).

2.4. Hydrologic Effects

Annual accumulation and concentrations of nonpoint source pollutants were modeled using the Open Nonpoint Source Pollution and Erosion Comparison Tool (OpenNSPECT) (Eslinger *et al.* 2012). OpenNSEPCT is an open-source Geographic Information Systems (GIS)-based tool that models pollutants and erosion loads delivered to coastal watersheds (NOAA 2012). OpenNSPECT relies on the relationship between land cover, nonpoint source pollutants, and erosion to estimate accumulations from overland flow within a watershed (NOAA 2012). Inputs to the model include elevation, land cover, rainfall, and soil data, R-factor, and pollutant coefficients.

Runoff is modeled as the basis for OpenNSPECT processes based on a methods developed by the National Resource Conservation Service (NRCS) (NRCS 1986). It relies on the inputs of rainfall, elevation, land cover and soil and produces an accumulated runoff grid output of volume in liters. Pollutant concentrations are estimated using land cover as an indirect means by which coefficients determined by water quality standards represent the contribution of each land cover class to overall pollutant load during a precipitation event (NOAA 2012). Five default pollutants are measured: nitrogen, phosphorus, total suspended

solids (TSS), lead, and zinc. Using pollutant coefficient values which represent an average concentration (mg/L) for each cell's land cover type and a flow direction grid from the DEM, a pollutant mass accumulation is calculated representing the accumulated pollutant mass at each cell and an accumulated pollutant concentration grid (Figure 2.2).

Rates of erosion and sediment loads are estimated with a modified version of the widely used revised universal soil loss equation (RUSLE) (Renard & Foster 1991):

$$A = R * K * L * S * C * \mathrm{P}$$

Where A is the average annual soil loss, R is a rainfall/runoff erosivity factor, K is a soil erosivity factor, L is the length-slope factor, S is the slope steepness factor, C is the cover management factor, and P is the support practice factor which is not included in the OpenNSPECT calculation (NOAA 2012). RUSLE uses these factors to represent the processes of infiltration, overland flow, particle detachment, and sediment transport (Larsen & MacDonald 2007). User inputs needed to model sediment yields include elevation, land cover, soils, and the rainfall/runoff erosivity factor (R factor). The output is a gridded annual accumulation of sediment yield.

OpenNSPECT is dependent upon land cover for predicting runoff, pollutants and erosion, therefore, changes in land cover inputs function primarily as a model sensitivity study. Model outputs based on changes in land cover were predicted by running OpenNSPECT for each year from 2005 to 2012. To accomplish this, each year an updated land cover dataset was used which incorporates the effects of fire in 2008. The years of 2005 – 2007 were years without fire or pre-fire years, 2008 included effects of the Basin Complex Fire, and 2009 – 2012 included both the Basin Complex and Chalk fires in post-fire years.

Hydrologic effects were measured at the basin level and also aggregated by burned and unburned. Sub-basins that were predominantly burned or unburned were delineated in order to more clearly separate burned and unburned areas. Partington Creek basin was divided into one unburned and one burned basin, and Limekiln Creek was divided into two unburned basins and one burned basin. All accumulation grids were overlapped with stream data and only channels that matched actual perennial and intermittent streams were considered for sampling. For all output grids, sample points or "pour points" where selected where streams drained into the ocean for 14 of the 15 basins (Figure 2.1). Brunette Creek basin drains into Arroyo De La Laguna basin before reaching the ocean, and therefore the two were merged and points were only taken from the pour point of Arroyo De La Laguna basin. Annual accumulation of loads and concentrations were gathered at each pour point. For analysis by basin, sample points were summed per basin then divided by the area of each basin to normalize for area. For comparing burned to unburned area, pour points were summed from basins where > 75 percent of the area burned (4 basins) and divided by the total area of burned basins. Likewise, the remaining 10 unburned basins were summed and divided by the total area of unburned.

2.5. Analysis

Impact of fire on hydrologic responses was visualized by comparing the percent change in modeled nonpoint source pollutants from burned and unburned basins from a pre-fire baseline (2005 – 2007) from all outputs from OpenNSPECT. In 2008, only the basins burned by the Basin Complex Fire were used to calculate the pre-fire baseline and the percent change in export. For all other years, all burned basins were included in the pre-fire baseline and the percent change in nonpoint source pollutants.

Spearman Rank correlation was used to explore the relationship between the changes in nonpoint source pollutants and the fire metrics. Percent changes in concentrations of each export per basin were compared to each fire metric for the two time periods (2006 – 2008 and 2006 – 2009). Percent change in basin nonpoint source pollutants for 2006 to 2008 and from 2006 to 2009 were correlated to Severity Metric (SM), High Severity (HS), and Forest Loss and Shrub Loss in 2008. Spearman Rank was used to account for the small sample size of basins (n = 14) and the non-normal distributions (Wilks 1995) Significance was measured at the $p < 0.05$ level.

3. Results

3.1. Land cover

Within fire perimeters, average pre fire (2005 – 2008) land cover proportions were 52 percent forest, 43 percent shrub and 5 percent grass (Figure 2.3). In 2008, after the Basin Complex Fire, grass cover increased to 46 percent as forest decreased to 11 percent with shrub maintaining at 43 percent. In 2009, approximately one year after both the Basin Complex and Chalk fires, forest decreases further to 8 percent of total cover, shrub increases to 76 percent and grass cover decreases to 16 percent. Post-fire land cover proportions (2010 – 2012) were 28 percent for forest cover, which increased slightly each post-fire year but still had less total cover than in pre-fire conditions. Shrub post-fire cover was 67 percent, which decreased each post-fire year but was still higher than pre-fire conditions. Average post-fire grass cover was 4 percent which was consistent with pre-fire grass cover.

3.2. Watershed Outputs

Modeled annual concentrations of phosphorus (P), Total Suspended Solids (TSS), and sediment summed within burned basins all increased above pre-fire baseline levels during 2008 (Figure 2.4) and 2009. There were was little change in nitrogen. Relative percent change in 2008 included only the basins affected by the Basin Complex Fire and showed that in 2008 there was 161 percent increase in phosphorus export, a 115 percent change in TSS, a 337 percent increase in sediment, and a 26 percent increase in runoff. In 2009, all of the burned basins had a 71 percent increase in phosphorus, a 53 percent increase in TSS, a 109 percent increase in sediment, and a 4 percent decrease in runoff over pre-fire baseline levels. For phosphorus, TSS, and sediment, pre- and post-fire levels were similar to those of unburned areas. Runoff, however, was higher in burned areas than in unburned areas pre-fire, but post-fire runoff dropped below that of unburned areas.

3.3 Burn severity and watershed export

Fire metrics were significantly correlated to relative change in nonpoint source pollutants at the $p < 0.01$ level (Table 2.2). The highest correlations for change between post-fire year 0 (2006 – 2008) were between Forest Loss and both phosphorus and sediment ($r = 0.89$, $p < 0.001$), and between SM and TSS ($r = 0.89$, $p < 0.001$). Overall, all of the fire metrics were strongly correlated with all of the relative changes in export, except for Forest Loss and runoff, which was not significant. The highest change between the post-fire year 1(2006 – 2009) period were between HS and phosphorus. For this period, runoff was not significantly correlated with any for the fire metrics. Omitting runoff, overall, for post-fire year 1, HS showed the strongest correlations with changes in export, while Forest Loss has the weakest correlations.

4. Discussion

The effects of the 2008 wildfire are shown in the observed land cover transitions and similar land cover changes have been observed in studies in comparable post-fire vegetation types. A reduction in forest and shrub cover in 2008 resulted in a large increase of grass cover which is due to the removal of shrub canopy promoting the growth of herbaceous annuals and perennials (Davis & Borchert 2006; Keeley 2006a). Keeley, Fotheringham & Baer-Keeley (2005) observed that in post-fire California Mediterranean shrublands during the first spring post-fire, approximately 50 percent of post-fire cover was composed of herbaceous annuals in the interior sage scrub communities and perennials in the coastal sage scrub.

In 2009, one year after both fires, shrub increases to 76 percent of the land cover. Shrub cover in California Mediterranean ecosystems consists of a variety of species that are obligate resprouters, obligate reseeders and facultative seeding species (Keeley 2006b). Coastal sage scrub communities are comprised of mostly commonly resprouters, while interior sage scrub is composed of fewer resprouting species and more facultative seeders that rely more on obligate seeding (Keeley 2006a). Dependent on slope and aspect, chaparral communities are a mixture of obligate seeders on xeric sites while resprouting species occupy more mesic sites (Keeley 2006a). All shrub species in this ecosystem are shown to regenerate in response to fire (Keeley 2006b) which is consistent with a large increase in shrub measured in 2009. Keeley, Fotheringham & Baer-Keeley (2005) also found that in a five-year study, shrub cover increased in each post-fire year, though shrub growth can vary post-fire (Keeley 1981). After 2009, there was subsequent decrease in shrub cover in every post-fire year (Figure 2) which could also be attributed to resprouting of coast live oak (Davis & Borchert 2006) that is classified as shrub initially, or spectral confusion between the shrub and

forest classes. These land cover transitions generally align with other studies that have shown that increasing density of vegetation decreases runoff (Nicolau & Solé-Benet 1996; Garcia-Estringana *et al.* 2010) and the presence and type of forest greatly reduces erosion (Descroix, Viramontes & Vauclin 2001). In the three post-fire years after 2009, grass cover returned to pre-fire levels, whereas forest cover remained below pre-fire levels and shrub remained above.

OpenNSPECT pollutant coefficients produce highest mass and concentration outputs for grass out of the three cover classes, but are the same for shrub and forest. For some pollutant coefficients such as nitrogen, all three cover classes produce the same mass and volume, making the model insensitive to changes in land cover for certain pollutants. This is also why modeled nitrogen did not show any significant changes between years. The increase of grass above pre-fire levels (and subsequent decrease in forest and shrub) in 2008 and to a lesser extent in 2009 is therefore the driving cause of increases in modeled pollutants. By 2012, percent change in nonpoint source pollutant levels are near or below pre-fire levels, though post-fire vegetation proportions differ from pre-fire.

When comparing the changes in nonpoint source pollutants by basin, those with the highest indications of fire severity also showed the largest modeled increases in nonpoint source pollutants. This indicates that increased burn severity is linked to certain land cover transitions. Higher levels of burn severity are associated with greater loss of forest and shrub and increases in grass to produce increases in nonpoint source pollutants, while unburned basins or basins low fire metric values showed less increase in pollutants and greater forest and shrub loss. Major transitions (i.e. from forest to grass) are occurring at the higher values of dNBR (Figure 2.5) compared to transitions between forest and shrub and shrub to grass.

The severity of a fire is one of the most important influences on post-fire erosion rates in many ecosystems (De Dios Benavides-Solorio & MacDonald 2005). Likewise, the highest levels of dNBR lead to changes in land cover that produced increased modeled changes in nonpoint source pollutants.

The use of a multi-year land cover dataset helped to explicate the impacts of the 2008 wildfires through changes in land cover and subsequent increases in modeled nonpoint source pollutants to the nearshore ecosystem above non fire years. These are effects that would not have been observed using only pre-fire land cover data. Various studies using in-situ stream measurements have found increases in watershed transport of nutrients in storm events after a fire. Hauer and Spencer (1998) collected stream nutrient data during a fire from a series of paired watersheds in Montana. Their results for concentrations are 5 to 10 fold higher for phosphorus and 13 to 25 fold higher for TSS. In southern California coastal watersheds, Stein et al. (2012) found a 921 fold increase in phosphorus concentration and a two fold increase in TSS after post-fire storm events. Our modeled annual phosphorus concentrations showed a 161 percent increase compared to pre-fire average and a 114 percent increase in TSS over a pre-fire average. Modeled increases are expected to be lower as they are measured over an annual scale. Studies have also found significant increases in sediment export during early season storms in southern California (Warrick *et al.* 2012; Coombs & Melack 2013) which corresponds to the 350 percent modeled annual increase in sediment in the fire year.

Though results agree with studies in finding orders of magnitude increases in nonpoint source pollutants post-fire, modeled concentrations tended to overestimate concentrations of nonpoint source pollutants compared to studies in similar areas (Warrick *et al.* 2012) or to

ecosystem specific water quality standards (US EPA 2000). Modeled phosphorus concentration in unburned years were about 5 times higher than ambient water quality criteria developed for the southern and central California chaparral and oak woodlands. The cause of this disagreement between concentrations can potentially be attributed to difference between spatial and temporal extents. Often post-fire runoff studies lack spatial and temporal context for reported result (Shakesby & Doerr 2006). The same is likely true for water quality standards generated at local and regional scales. Studies collecting *in-situ* stream data are also primarily conducted in response to individual storm events, while our modeled data are based on an annual average of precipitation with no extremes; responses are averaged throughout the year.

Along with challenges of comparison with *in-situ* studies, several limitations have been observed. The model is primarily for small and mostly urban watersheds (NOAA 2012). First, there are also inaccuracies inherent in each of the data inputs. For land cover data, accuracy is spatially heterogeneous, making it difficult to pinpoint specific locations of errors. Second, Larson & MacDonald (2007) tested the accuracy of two annual time scale models: the physically based Disturbed WEPP and empirically based RUSLE models to predict post-fire sediment yields in the Colorado Front Range and found that they were poorly correlated to actual sediment yields. The RUSLE model, designed to predict long-term annual averages of soil loss for conservation planning and assessment, does not account for sediment in channels and is more appropriate for small areas (Nearing *et al.* 2005). Finally, precipitation inputs into OpenNSPECT for each year were for the 30 year climatological normal, however, precipitation is a major driver of watershed responses (Moody *et al.* 2013) and the variation in observed annual precipitation would produce differing amounts of runoff each year. The years

2007 through 2009 included a droughty period with below normal precipitation, which was likely a primary driver of the fire activity, and could have had a variety of effects on land cover independent of the fires.

True post-fire conditions could not be reflected in model processes and inputs. Post-fire runoff is relatively poorly understood (Moody et al 2013; Stein et al 2012) especially in California chaparral watersheds (Coombs & Melack 2013). Land cover data is represented as static through the year in the model, however, in post-fire environments there are interannual changes in fire year vegetation. It is likely that during the first storm event after the fire, vegetation cover is sparser but continues to grow throughout the rainy season. Sparser vegetation cover would lead to increased export (Robichaud, Beyers & Neary 2000) especially considering the effects of fire on soils. Severe wildfire produces highly spatially variable hydrophobic soils in California chaparral (Hubbert *et al.* 2006) which is not accounted for in the soil dataset. The Basin Complex Fire produced various degrees of soil hydrophobicity within high and moderate soil burn severity ratings (SEAT 2008). Also, combustion of plants and other natural materials releases nutrients present in ash (Ranalli 2004) in ways that are distinct from runoff from agricultural or developed land cover and are not accounted for in OpenNSPECT. Wildfire creates an increases in nutrients such as phosphorus and nitrogen primarily through smoke and the deposition of ash through overland flow (Ranalli 2004).

5. Management Implications

Despite these limitations and uncertainties, our modeled increases in nonpoint source pollutants correspond with post-fire research by generally showing increases in runoff, sediment, and nutrients. We hypothesize that results would not be significantly altered due to the sensitivity of the model to land cover transitions resulting from the 2008 fires. Due to additional source of nutrients not modeled through OpenNSPECT, we believe that this model produces a conservative estimate of the export of nutrients and sediment from these coastal watersheds. A water quality management plan for a watershed in just south of Big Sur Morro Bay indicates that sediment loading is 50 percent higher than the established total maximum daily load (TMDL) and would be even higher in the event of a wildfire in the basin (State of California Central Coast Regional Water Quality Control Board 2002). Our modeled results indicate a 350 percent increase in sediment yield. An increase of this magnitude violates these established water quality standards from nearby coastal watersheds. Although central California coastlines are relatively unimpaired (Green *et al.* 2004) nutrient loading and the growth of toxic algae has been documented to cause sea otters mortality in Monterey Bay (Miller *et al.* 2010). Though we modeled a 161 percent increase in phosphorus, these elevated levels were fleeting, returning to pre-fire levels two years after fire. This may not be enough of an increase to create impaired coastal waters, however incorporating more representative post-fire parameters, such as soil hydrophobicity, annual precipitation, and additional land cover classes would likely lead to higher levels of increase than modeled.

Climate impacts have shown to be increasing the severity of fires across California (Miller & Safford 2012) as well as fire occurrence in California (Westerling & Bryant 2008). For weather-driven fire on the central California coast (Moritz 1997) increasing temperatures

could lead to lead to further increases in wildfire activity. Although it is uncertain how precipitation may change regionally across California within the next century (Cayan *et al.* 2008) the sensitivity of the modeled output to changes in land cover indicate that increases in nonpoint source pollutants to the nearshore are coupled with increased occurrence and severity of wildfire.

Coastal California water quality management plans include the marine ecosystem as a "beneficial use" (State of California Central Coast Regional Water Quality Control Board 2002) while post-fire emergency assessments do not (SEAT 2008; USDA Forest Service 2010). A wildfire occurring within the in Morro Bay south of Big Sur is considered a situation in which water quality standards (TMDLs) are will not be met (State of California Central Coast Regional Water Quality Control Board 2002). Therefore, it should also be important to consider the nearshore ecosystem as a "value at risk" for fire-prone coastal wildland areas.

6. Conclusion

Understanding the impacts of increases in wildfire on ecosystems is important especially when considering coupled ecosystems of coastal watersheds and the nearshore environment. Recent research has shown the effects of fire on a threatened marine mammal in the nearshore ecosystem and fires that burn in watersheds adjacent to nearshore ecosystems impact the marine habitat by increasing nonpoint source pollutants above pre-fire levels. This research links the severity of wildfire to land cover changes that subsequently increase exports of pollutants and sediment to the nearshore environment. Not only is it replicable across other watersheds, it also indicates that terrestrial land management revolving around wildfire, including suppression, thinning, post-fire rehabilitation, and other activities changing land

cover at a landscape scale, can be assessed for potential impacts to the nearshore environment. Coupling terrestrial and nearshore marine ecosystems in such a way may provide considerable insight to terrestrial impacts on the health and welfare of marine species at risk.

Figures & Tables

Figure 2.1. Basins and sample points in the Big Sur region of coastal central California. Burned basins are in bold.

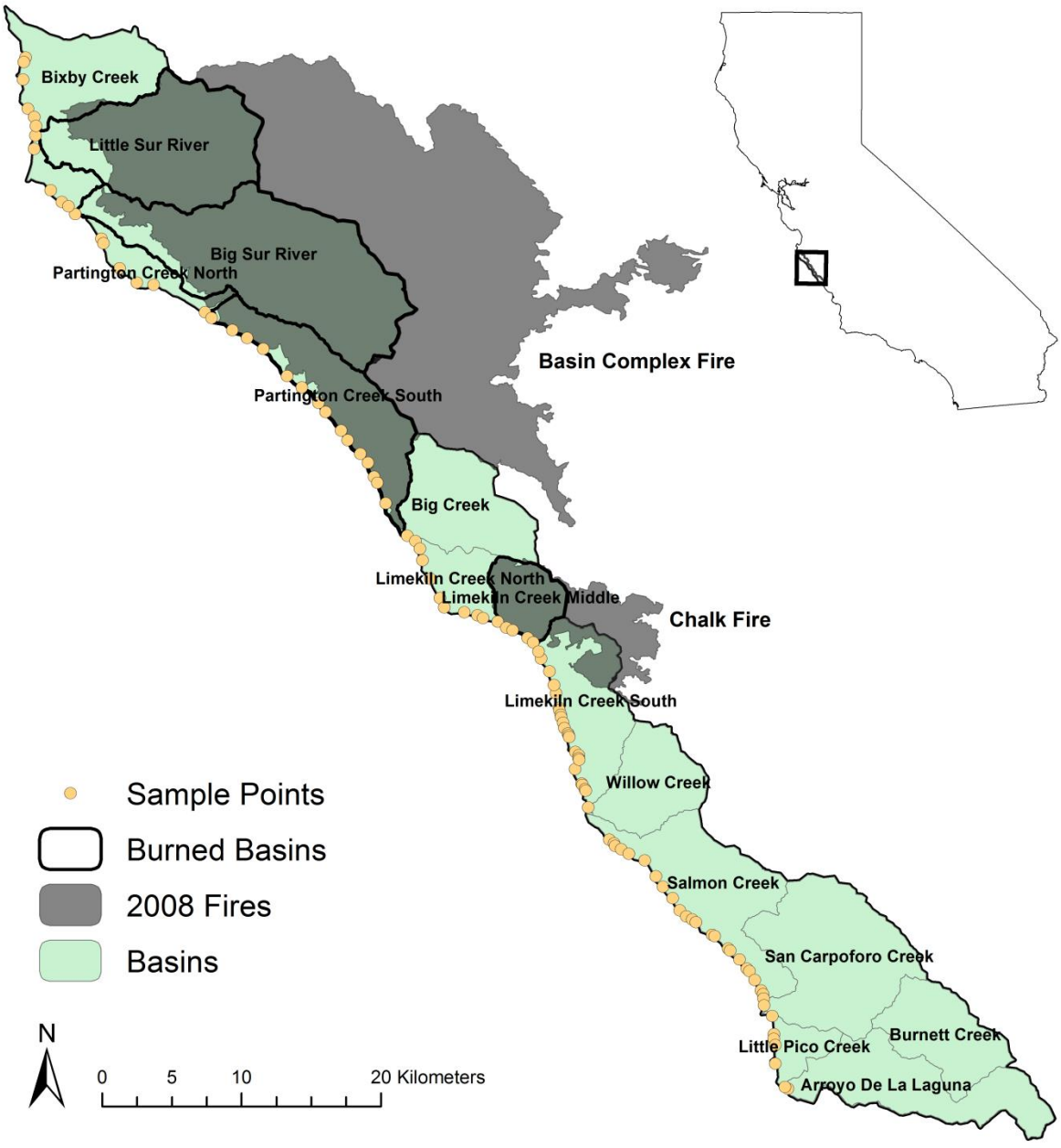

Figure 2.2. OpenNSPECT pollutant concentration estimation process (NOAA 2012). Shading represents output dataset (continued on next page).

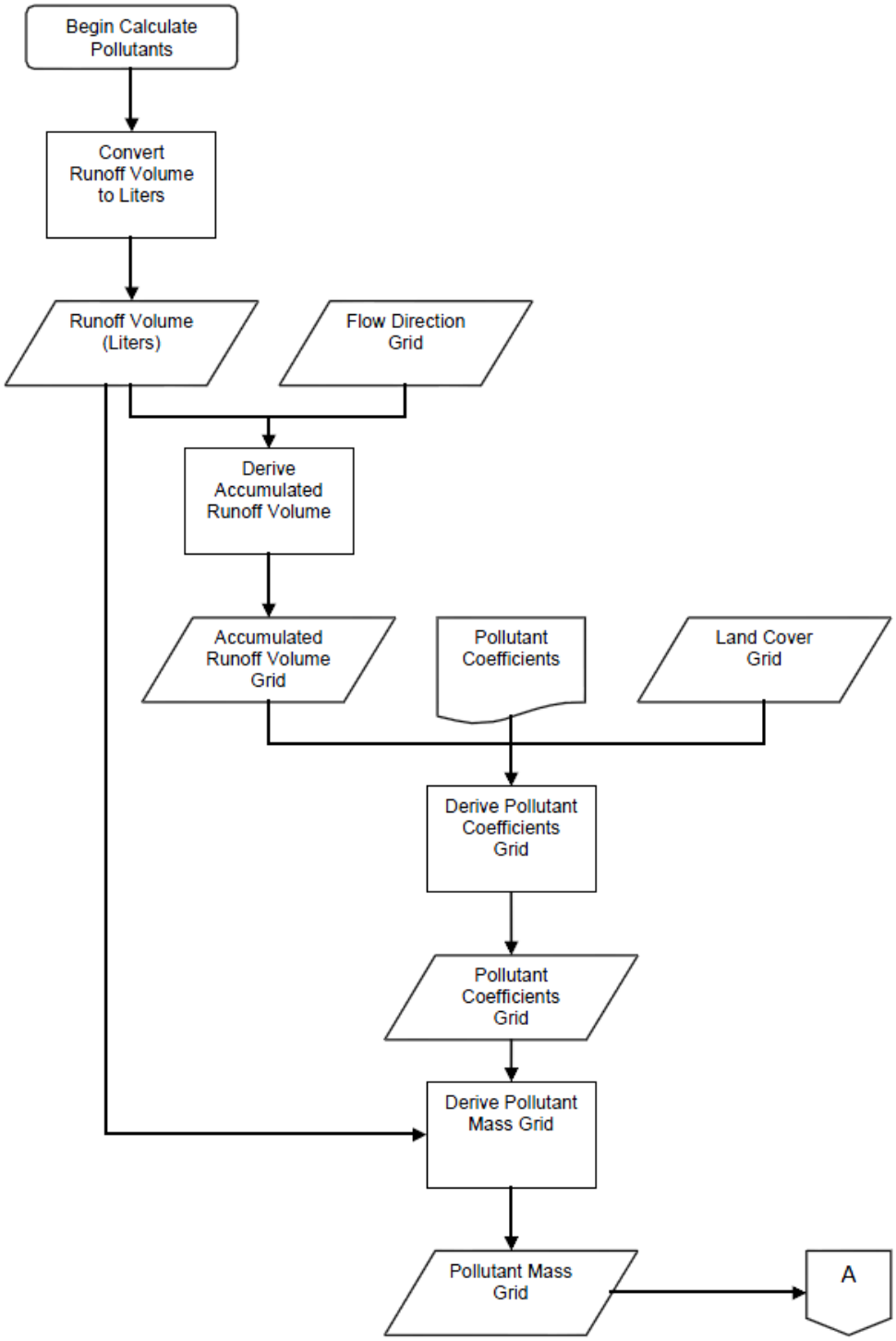

Figure 2.2. OpenNSPECT pollutant concentration estimation process (NOAA 2012). Shading represents output dataset (continued from previous page).

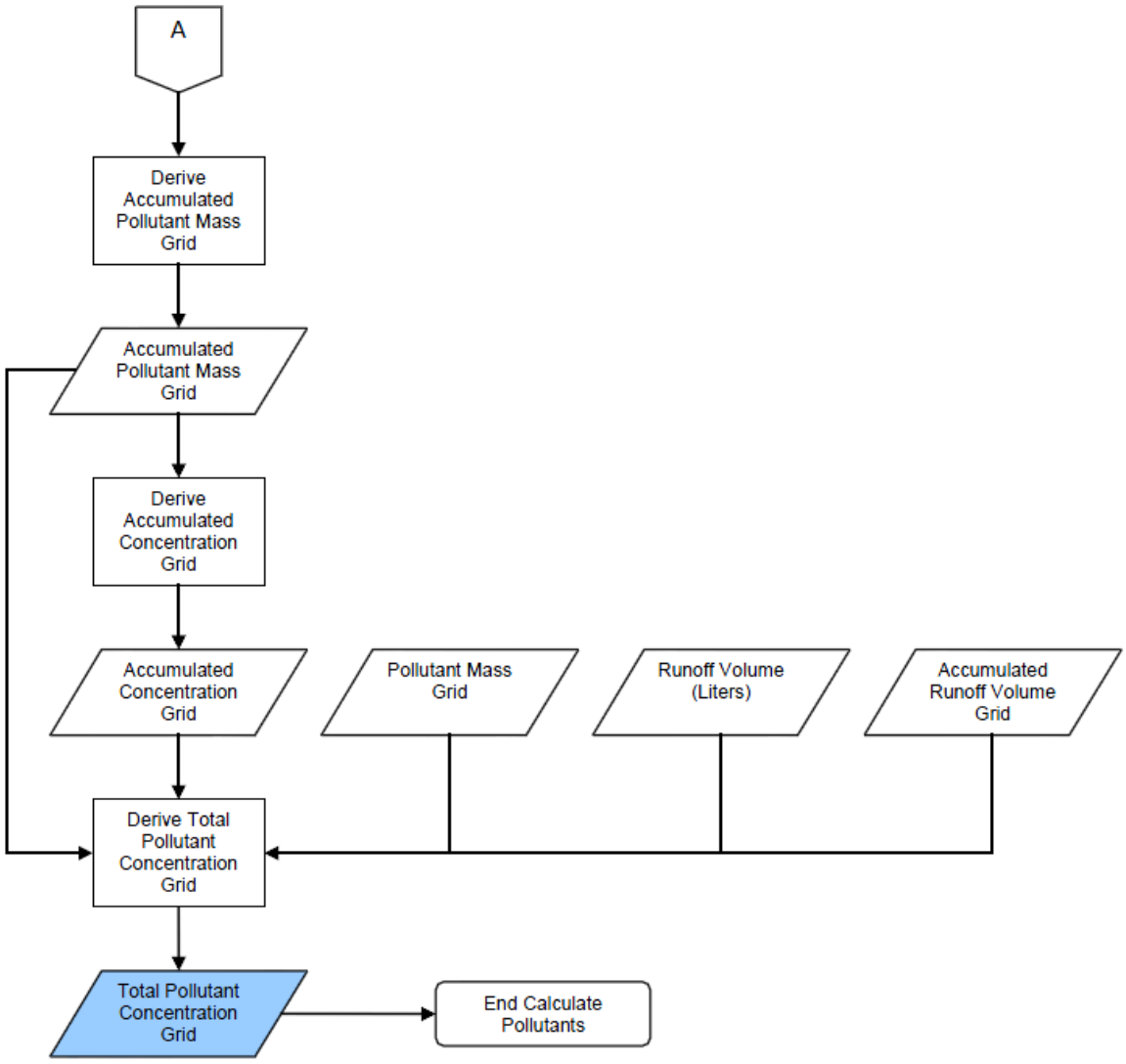

Figure 2.3. Burned and unburned land cover transitions in (a.) forest, (b.) shrub, and (c.) grass cover over the study period (2005 – 2012). Envelopes represent the average error of commission as a percent for each class.

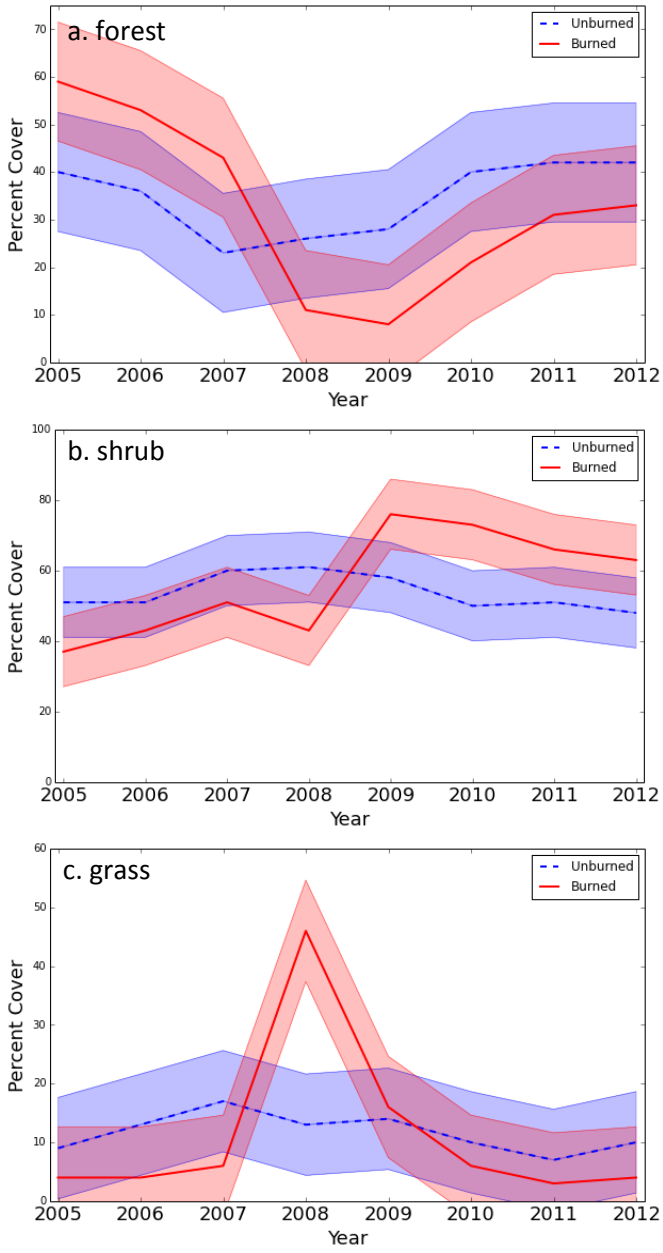

Figure 2.4. Percent change in export based on pre-fire average (2005 – 2007) for both burned and unburned basins. Within burned areas, 2008 only includes the burned basins and pre-fire baseline from basin affected by the Basin Complex fire.

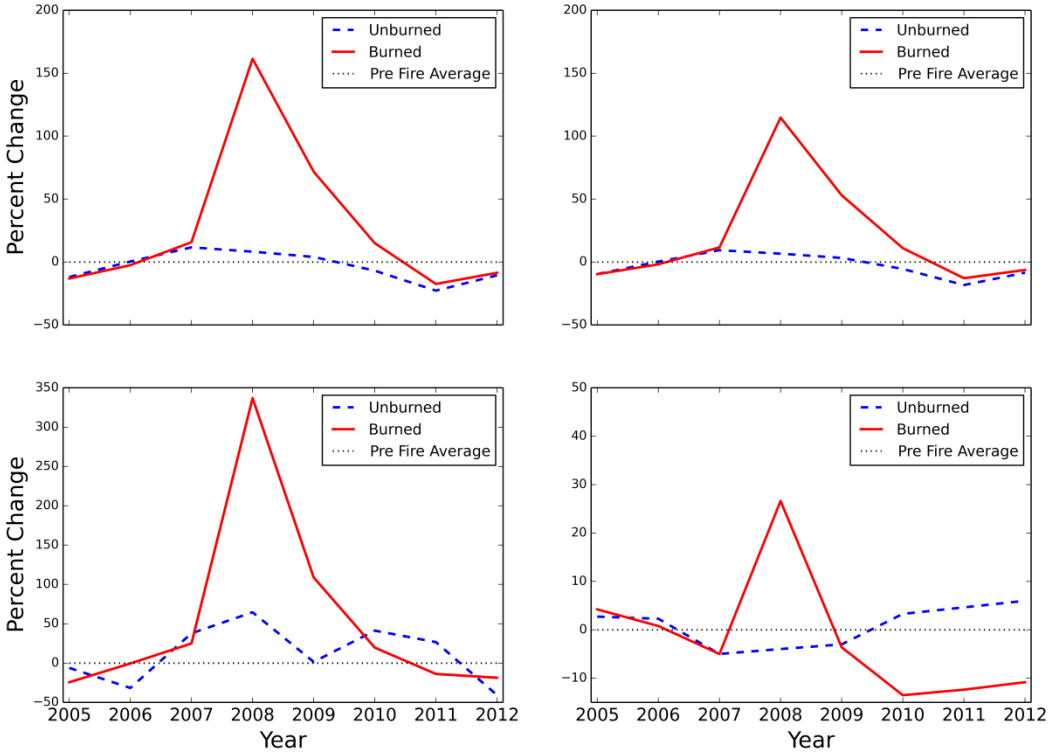

Figure 2.5. Distributions of dNBR per land cover transition. FG = forest to grass, FS = forest to shrub, and SG = shrub to grass.

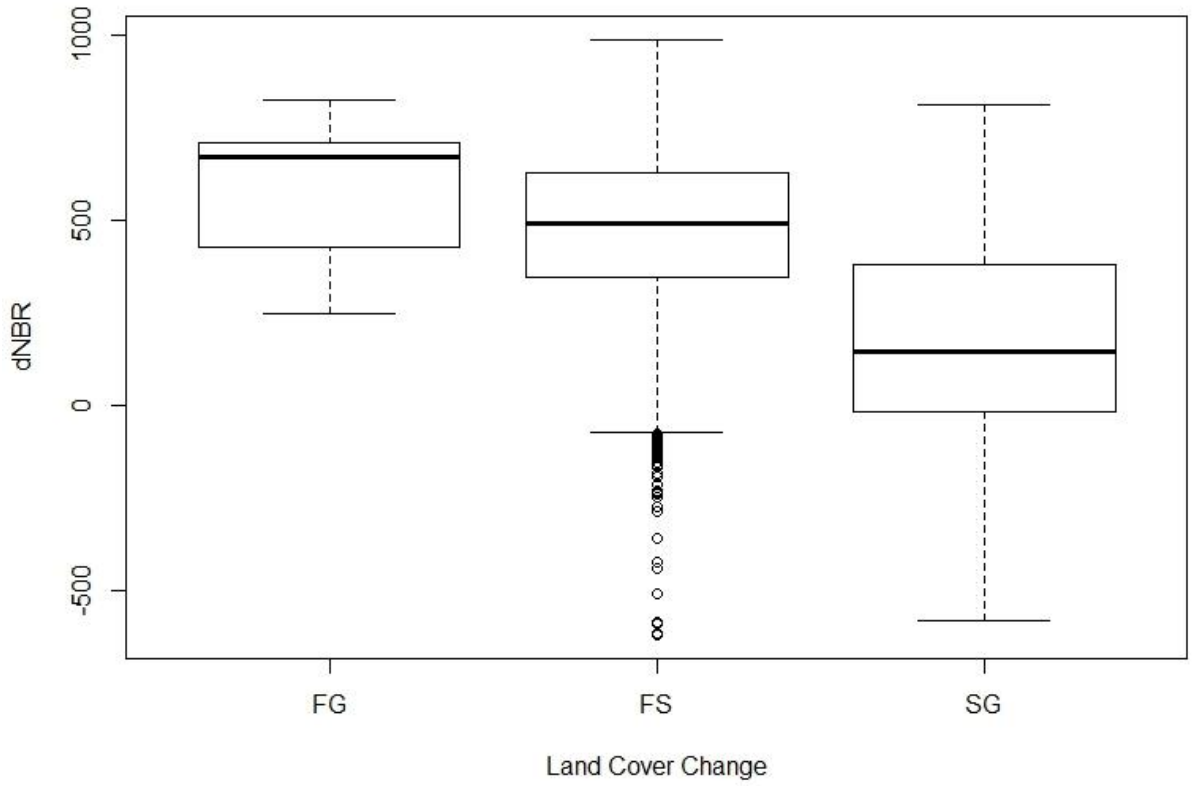

Table 2.1. Basins within the study area from north to south and fire impacts including fire name, percent area burned, percent high severity (calculated as percent high severity of percent area burned), and Severity Metric (SM). Basins in bold are considered to be the burned basins for analysis and were > 75 % burned.

Basin	Area (km2)	Fire	% Area Burned	% High Severity (HS)	SM
Bixby Creek	66.2	Basin	3.5	1.8	0.3772
Little Sur River	102.9	Basin	87.1	39.1	0.3954
Big Sur River	148.5	Basin	91.9	38.0	0.3783
Partington Creek North	16.5	Basin	9.5	0.2	0.178
Partington Creek South	65.1	Basin	92.5	29.5	0.3283
Big Creek	55.7	Basin/Chalk	1.0	0.2	0.2892
Limekiln Creek North	22.0	Chalk	1.4	0.3	0.3209
Limekiln Creek Middle	23.7	Chalk	98.8	19.4	0.2903
Limekiln Creek South	52.2	Chalk	21.8	7.4	0.3545
Willow Creek	41.0		0	0	0
Salmon Creek	70.3		0	0	0
San Carpoforo Creek	90.6		0	0	0
Little Pico Creek	14.2		0	0	0
Arroyo De La Laguna/ Burnett Creek	107.9		0	0	0

Table 2.2. Spearman Rank correlations (r) between fire metrics and percent changes in modeled annual concentrations of nonpoint source pollutants for the two periods of post-fire year 0 (2006 – 2008) and post-fire year 1 (2006 – 2009). Values in bold are significant at the $p < 0.01$ level.

Post-fire year 0

	Δ Phosphorus	Δ TSS	Δ Sediment	Δ Runoff
HS	**0.82**	**0.83**	**0.75**	**0.72**
SM	**0.75**	**0.89**	**0.76**	**0.75**
FL	**0.89**	**0.84**	**0.89**	0.44
SL	**0.72**	**0.81**	**0.73**	**0.88**

Post-fire year 1

	Δ Phosphorus	Δ TSS	Δ Sediment	Δ Runoff
HS	**0.88**	**0.87**	**0.87**	0.33
SM	**0.82**	**0.81**	**0.85**	0.37
FL	**0.76**	**0.76**	**0.78**	0.09
SL	**0.81**	**0.84**	**0.82**	0.28

References

Bodkin, J., Ballachey, B., Dean, T., Fukuyama, A., Jewett, S., McDonald, L., Monson, D., O'Clari, C. & VanBlaricom, G. (2002) Sea otter population status and the process of recovery from the 1989 "Exxon Valdez"oil spill. *Marine Ecology Progress Series*, **241**, 237–253.

Bowen, L., Miles, A., Kolden, C., Saarinen, J., Murray, M. & Tinker, T. (2014) Effects of wildfire on sea otter (Enhydra lutris) immune function. *Marine Mammal Science*.

California Department of Water Resources. (2010) *California's Drought of 2007 – 2009: An Overview*.

Callaway, R. & Davis, F. (1993) Vegetation dynamics, fire, and the physical environment in coastal central California. *Ecology*, **74**, 1567–1578.

Cayan, D.R., Maurer, E.P., Dettinger, M.D., Tyree, M. & Hayhoe, K. (2008) Climate change scenarios for the California region. *Climatic Change*, **87**, 21–42.

Congalton, R.G.R. (1991) A review of assessing the accuracy of classifications of remotely sensed data. *Remote Sensing of Environment*, **46**, 35–46.

Conrad, P.A., Miller, M.., Kreuder, C., James, E.R., Mazet, J., Dabritz, H., Jessup, D.A., Gulland, F. & Grigg, M.E. (2005) Transmission of Toxoplasma: clues from the study of sea otters as sentinels of Toxoplasma gondii flow into the marine environment. *International journal for parasitology*, **35**, 1155–68.

Coombs, J.S. & Melack, J.M. (2013) Initial impacts of a wildfire on hydrology and suspended sediment and nutrient export in California chaparral watersheds. *Hydrological Processes*, **27**, 3842–3851.

Davis, F.W. & Borchert, M.I. (2006) Central Coast Bioregion. *Fire in Californa's Ecosystems* (eds N.G. Sugihara, J.W. Wagtendonk, K.E. Shaffer, J. Fites-Kaufman & A.E. Thode), p. 596. University of California Press.

Davis, F.W., Borchert, M., Meentemeyer, R.K., Flint, A. & Rizzo, D.M. (2010) Pre-impact forest composition and ongoing tree mortality associated with sudden oak death in the Big Sur region; California. *Forest Ecology and Management*, **259**, 2342–2354.

Descroix, L., Viramontes, D. & Vauclin, M. (2001) Influence of soil surface features and vegetation on runoff and erosion in the Western Sierra Madre (Durango , Northwest Mexico). *Catena*, **43**, 115–135.

Dillon, G.K., Holden, Z.A., Morgan, P., Crimmins, M.A., Heyerdahl, E.K. & Luce, C.H. (2011) Both topography and climate affected forest and woodland burn severity in two regions of the western US, 1984 to 2006. *Ecosphere*, **2**, art130.

De Dios Benavides-Solorio, J. & MacDonald, L.H. (2005) Measurement and prediction of post-fire erosion at the hillslope scale, Colorado Front Range. *International Journal of Wildland Fire*, **14**, 457.

Dowd, B., Press, D. & Huertos, M. (2008) Agricultural nonpoint source water pollution policy: The case of California's Central Coast. *Agriculture, Ecosystems & Environment*, **128**, 151–161.

Elliot, W.J. & Hall, D.E. (2010) Disburbed WEPP Model 2.0 Ver. 2014.04.14 Moscow, ID. *USDA Forest Service Rocky Mountain Research Station Online at <http://forest.moscowfsl.wsu.edu/fswepp>*.

Epting, J., Verbyla, D. & Sorbel, B. (2005) Evaluation of remotely sensed indices for assessing burn severity in interior Alaska using Landsat TM and ETM+. *Remote Sensing of Environment*, **96**, 328–339.

Eslinger, D.L., Carter, H.J., Pendleton, M., Burkhalter, S. & Allen, M. (2012) OpenNSPECT: The Open-source Nonpoint Source Pollution and Erostion Comparison Tool.

Fites-Kaufman, J., Bradley, A.F. & Merrill, A.G. (2006) Fire and Plant Interactions. *Fire in Californa's Ecosystems* (eds N.G. Sugihara, J.W. van Wagtendonk, K.E. Shaffer, J. Fites-Kaufman & A.E. Thode), p. 596. University of California Press.

Foody, G.M. (2002) Status of land cover classification accuracy assessment. *Remote Sensing of Environment*, **80**, 185–201.

Garcia-Estringana, P., Alonso-Blázquez, N., Marques, M.J., Bienes, R. & Alegre, J. (2010) Direct and indirect effects of Mediterranean vegetation on runoff and soil loss. *European Journal of Soil Science*, **61**, 174–185.

Goodridge, B.M. & Melack, J.M. (2012) Land use control of stream nitrate concentrations in mountainous coastal California watersheds. *Journal of Geophysical Research: Biogeosciences*, **117**, 1–17.

Green, P. a., Vörösmarty, C.J., Meybeck, M., Galloway, J.N., Peterson, B.J. & Boyer, E.W. (2004) Pre-industrial and contemporary fluxes of nitrogen through rivers: a global assessment based on typology. *Biogeochemistry*, **68**, 71–105.

Greenlee, J. & Langenheim, J. (1990) Historic fire regimes and their relation to vegetation patterns in the Monterey Bay area of California. *American Midland Naturalist*, **124**, 239–253.

Gresswell, R. (1999) Fire and aquatic ecosystems in forested biomes of North America. *Transactions of the American fisheries society*, **128**, 37–41.

Hauer, F. & Spencer, C. (1998) Phosphorus and nitrogen dynamics in streams associated with wildfire: a study of immediate and longterm effects. *International Journal of Wildland Fire*, **8**, 183–198.

Hubbert, K.R., Preisler, H.K., Wohlgemuth, P.M., Graham, R.C. & Narog, M.G. (2006) Prescribed burning effects on soil physical properties and soil water repellency in a steep chaparral watershed, southern California, USA. *Geoderma*, **130**, 284–298.

Jensen, J.R. (1983) Review Article: Biophysical Remote Sensing. *Annals of the Association of American Geographers*, **73**, 111–132.

Jensen, J.R. (2007) *Remote Sensing of the Environment An Earth Resource Perspective*, 2nd ed. Pearson Prentice Hall.

Johnson, C.K., Tinker, M.T., Estes, J. a, Conrad, P. a, Staedler, M., Miller, M. a, Jessup, D. a & Mazet, J. a K. (2009) Prey choice and habitat use drive sea otter pathogen exposure in a resource-limited coastal system. *Proceedings of the National Academy of Sciences of the United States of America*, **106**, 2242–7.

Keeley, J.E. (2006a) South Coast Bioregion. *Fire in Californa's Ecosystems* (eds N.G. Sugihara, J.W. van Wagtendonk, K.E. Shaffer, J. Fites-Kaufman & A.E. Thode), p. 596. University of California Press.

Keeley, J. (2006b) Demographic patterns of postfire regeneration in Mediterranean-climate shrublands of California. *Ecological Monographs*, **76**, 235–255.

Keeley, J.E.J., Brennan, T. & Pfaff, A.A.H. (2008) Fire severity and ecosytem responses following crown fires in California shrublands. *Ecological applications : a publication of the Ecological Society of America*, **18**, 1530–46.

Keeley, J., Fotheringhap, C.J. & Baer-Keeley, M. (2005) Determinants of postfire recovery and succession in Mediterranean-climate shrublands of California. *Ecological Applications*, **15**, 1515–1534.

Keeley, J. & Zedler, P. (1978) Reproduction of chaparral shrubs after fire: a comparison of sprouting and seeding strategies. *American Midland Naturalist*, **99**, 142–161.

Keeley, J.E. & Zedler, P.H. (2009) Large, high-intensity fire events in southern California shrublands: debunking the fine-grain age patch model. *Ecological applications : a publication of the Ecological Society of America*, **19**, 69–94.

Key, C. & Benson, N. (2006) Landscape assessment (LA): Sampling and Analysis methods. *USDA Forest Service Gen. Tech. Rep. RMRS-GTR-164-CD*, 55.

Kolden, C. a. & Abatzoglou, J.T. (2012) Wildfire Consumption and Interannual Impacts by Land Cover in Alaskan Boreal Forest. *Fire Ecology*, **7**, 98–114.

Larsen, I.J. & MacDonald, L.H. (2007) Predicting postfire sediment yields at the hillslope scale: Testing RUSLE and Disturbed WEPP. *Water Resources Research*, **43**, 1–18.

Lentile, L. (2005) Patch structure, fire-scar formation, and tree regeneration in a large mixed-severity fire in the South Dakota Black Hills, USA. *Canadian Journal of Forest Resources*, **35**, 2875–2885.

Littell, J., McKenzie, D., Peterson, D.L. & Westerling, A.L. (2009) Climate and wildfire area burned in western US ecoprovinces, 1916-2003. *Ecological Applications*, **19**, 1003–1021.

Lutz, J., Key, C., Kolden, C., Kane, J.T. & Wagtendonk, J.W. van. (2011) Fire frequency, area burned, and severity: a quantitative approach to defining a normal fire year. *Fire Ecology*, **7**, 51–65.

Miller, M. a, Kudela, R.M., Mekebri, A., Crane, D., Oates, S.C., Tinker, M.T., Staedler, M., Miller, W. a, Toy-Choutka, S., Dominik, C., Hardin, D., Langlois, G., Murray, M., Ward, K. & Jessup, D. a. (2010) Evidence for a novel marine harmful algal bloom: cyanotoxin (microcystin) transfer from land to sea otters. *PloS one*, **5**.

Miller, J.D. & Safford, H. (2012) Trends in Wildfire Severity: 1984 To2010 in the Sierra Nevada, Modoc Plateau, and Southern Cascades, California, Usa. *Fire Ecology*, **8**, 41–57.

Miller, J.D. & Thode, A.E. (2007) Quantifying burn severity in a heterogeneous landscape with a relative version of the delta Normalized Burn Ratio (dNBR). *Remote Sensing of Environment*, **109**, 66–80.

Moody, J. a., Shakesby, R. a., Robichaud, P.R., Cannon, S.H. & Martin, D. a. (2013) Current research issues related to post-wildfire runoff and erosion processes. *Earth-Science Reviews*, **122**, 10–37.

Moritz, M. (1997) Analyzing extreme disturbance events: fire in Los Padres National Forest. *Ecological Applications*, **7**, 1252–1262.

Myers, N., Mittermeier, R. a, Mittermeier, C.G., da Fonseca, G. a & Kent, J. (2000) Biodiversity hotspots for conservation priorities. *Nature*, **403**, 853–8.

Nearing, M.A., Jetten, V., Baffaut, C., Cerdan, O., Couturier, A., Hernandez, M., Le Bissonnais, Y., Nichols, M.H., Nunes, J.P., Renschler, C.S., Souchere, V. & van Oost, K. (2005) Modeling response of soil erosion and runoff to changes in precipitation and cover. *Catena*, **61**, 131–154.

Nicolau, J. & Solé-Benet, A. (1996) Effects of soil and vegetation on runoff along a catena in semi-arid Spain. *Geomorphology*, **14**, 297–309.

NOAA. (2012) National Oceanic and Atmospheric Administration. Technical Guide for OpenNSPECT, Version 1.1. http://www.csc.noaa.gov/digitalcoast/tools/opennspect. , 44.

NRCS. (1986) Urban Hydrology for Small Watersheds TR-55. *USDA Natural Resource Conservation Service Conservation Engeneering Division Technical Release 55*, 164.

Ranalli, A. (2004) A summary of the scientific literature on the effects of fire on the concentration of nutrients in surface waters. *USDI Geological Survey Open-File Report 2004-1296*, 23.

Renard, K. & Foster, G. (1991) RUSLE: Revised universal soil loss equation. *Journal of soil and Water Conservation*, **46**.

Renschler, C.S. (2003) Designing geo-spatial interfaces to scale process models: the GeoWEPP approach. *Hydrological Processes*, **17**, 1005–1017.

Robichaud, P., Beyers, J. & Neary, D. (2000) Evaluating the effectiveness of postfire rehabilitation treatments. *USDA Forest Service Rocky Mountain Research Station General Technical Report RMSR-GTR-63*, 89.

Robichaud, P.R., Elliot, W.J., Pierson, F.B., Hall, D.E., Moffet, C.A. & Ashmun, L.E. (2007) Erosion Risk Management Tool (ERMiT) User Manual. *USDA Forest Service Rocky Mountain Research Station General Technical Report RMRS-GTR-188*, 31.

Santana, V.M., Baeza, M.J. & Maestre, F.T. (2012) Seedling establishment along post-fire succession in Mediterranean shrublands dominated by obligate seeders. *Acta Oecologica*, **39**, 51–60.

SEAT. (2008) State Emergency Assessment Team. Basin-Indians Fire Affecting Watersheds in Monterey County California, 120.

Shakesby, R. & Doerr, S. (2006) Wildfire as a hydrological and geomorphological agent. *Earth-Science Reviews*, **74**, 269–307.

Smith, A.M.S., Wooster, M.J., Drake, N. a., Dipotso, F.M., Falkowski, M.J. & Hudak, A.T. (2005) Testing the potential of multi-spectral remote sensing for retrospectively estimating fire severity in African Savannahs. *Remote Sensing of Environment*, **97**, 92–115.

Spencer, C.N. & Hauer, F.R. (1991) Phosphorus and Nitrogen Dynamics in Streams during a Wildfire Phosphorus. *Journal of the North Americal Benthological Society*, **10**, 24–30.

State of California Central Coast Regional Water Quality Control Board. (2002) Morro Bay Total Maximum Daily Load for Sediment (including Chorro Creek , Los Osos Creek and the Morro Bay Estuary). , 88.

Stein, E.D., Brown, J.S., Hogue, T.S., Burke, M.P. & Kinoshita, A. (2012) Stormwater contaminant loading following southern California wildfires. *Environmental toxicology and chemistry*, **31**, 2625–38.

U.S. Fish & Wildlife Service. (2014) Southern Sea Otter Information, http://www.fws.gov/Ventura/species_information/so_sea_otter/index.html

U.S. Geological Survey. (2014) Multi-Resolution Characteristics Consortium (MLCR), http://www.mrlc.gov/index.php

US EPA. (2000) Ambient Water Quality Criteria Recommendations of State and Tribal Nutrient Criteria Rivers and Streams in Nutrient Ecoregion III. *US Environmental Protection Agency EPA 822-B-00-016*, 70.

USDA Forest Service. (2010) Station Fire BAER Revisit. *USDA Forest Service Pacific Southwest Region Angeles National Forest*, 70.

Venn-Watson, S., Smith, C.R., Jensen, E.D. & Rowles, T. (2013) Assessing the potential health impacts of the 2003 and 2007 firestorms on bottlenose dolphins (Trusiops trucatus) in San Diego. *Inhalation toxicology*, **29**, 481–491.

Warrick, J.A., Hatten, J.A., Pasternack, G.B., Gray, A.B., Goni, M.A. & Wheatcroft, R.A. (2012) The effects of wildfire on the sediment yield of a coastal California watershed. *Geological Society of America Bulletin*, **124**, 1130–1146.

Westerling, A.L. & Bryant, B.P. (2008) Climate change and wildfire in California. *Climatic Change*, **87**, 231–249.

Westerling, A.L., Hidalgo, H.G., Cayan, D.. R. & Swetnam, T.W. (2006) Warming and earlier spring increase western U.S. forest wildfire activity. *Science*, **313**, 940–3.

Wilks, D.S. (1995) *Statistical Methods in the Aptmosperic Sciences*. Academic Press, San Diego, Ca.